

DEL-1 promotes macrophage efferocytosis and clearance of inflammation

Ioannis Kourtzelis^{1,2,13*}, Xiaofei Li^{3,13}, Ioannis Mitroulis^{1,2}, Daniel Grosser^{4,5}, Tetsuhiro Kajikawa³, Baomei Wang³, Michal Grzybek^{4,5}, Janusz von Renesse¹, Aleksander Czogalla⁶, Maria Troullinaki¹, Anaisa Ferreira¹, Christian Doreth¹, Klara Ruppova¹, Lan-Sun Chen¹, Kavita Hosur³, Jong-Hyung Lim¹, Kyoung-Jin Chung^{1,4,5}, Sylvia Grossklaus¹, Anne Kathrin Tausche⁷, Leo A. B. Joosten⁸, Niki M. Moutsopoulos⁹, Ben Wielockx¹⁰, Antonio Castrillo^{10,11}, Jonathan M. Korostoff¹², Ünal Coskun^{4,5}, George Hajishengallis^{3,14*} and Triantafyllos Chavakis^{1,14*}

Resolution of inflammation is essential for tissue homeostasis and represents a promising approach to inflammatory disorders. Here we found that developmental endothelial locus-1 (DEL-1), a secreted protein that inhibits leukocyte-endothelial adhesion and inflammation initiation, also functions as a non-redundant downstream effector in inflammation clearance. In human and mouse periodontitis, waning of inflammation was correlated with DEL-1 upregulation, whereas resolution of experimental periodontitis failed in DEL-1 deficiency. This concept was mechanistically substantiated in acute monosodium-urate-crystal-induced inflammation, where the pro-resolution function of DEL-1 was attributed to effective apoptotic neutrophil clearance (efferocytosis). DEL-1-mediated efferocytosis induced liver X receptor-dependent macrophage reprogramming to a pro-resolving phenotype and was required for optimal production of at least certain specific pro-resolving mediators. Experiments in transgenic mice with cell-specific overexpression of DEL-1 linked its anti-leukocyte-recruitment action to endothelial cell-derived DEL-1 and its efferocytic/pro-resolving action to macrophage-derived DEL-1. Thus, the compartmentalized expression of DEL-1 facilitates distinct homeostatic functions in an appropriate context that can be harnessed therapeutically.

Timely termination of an inflammatory response is of major importance to prevent unwarranted tissue damage and promote reconstitution of tissue integrity after sterile or microbial inflammatory insults¹. Resolution of acute neutrophilic inflammation^{1,2} requires a well-orchestrated series of processes, including downregulation of proinflammatory mediators, termination of further neutrophil recruitment, and clearance of neutrophils^{1,2}. In this regard, after performing acute proinflammatory actions, recruited neutrophils in the inflamed site undergo apoptosis and are cleared by macrophage phagocytosis through a process known as efferocytosis^{3,4}. Efficient engulfment of apoptotic neutrophils is mediated by specific macrophage receptors that directly or indirectly recognize the major 'eat-me' signal phosphatidylserine (PS) on the apoptotic cell surface^{5,6}. Resolving macrophages upregulate efferocytic receptors and opsonins that bridge them to apoptotic cells^{6,7}. Efferocytosis serves as more than waste disposal, as this process promotes a

pro-resolving phenotype in macrophages; defective efferocytic activity has been associated with persistence and chronicity of inflammation¹. Consistently, efferocytic macrophages release immunomodulatory molecules, such as transforming growth factor- β (TGF- β)^{6,7}.

Developmental endothelial locus-1 (DEL-1) is a secreted multi-functional protein that interacts with integrins⁸. DEL-1 comprises three N-terminal epidermal growth factor (EGF)-like repeats and two C-terminal discoidin I-like domains; hence, it is also known as EGF-like repeats and discoidin I-like domains 3 (EDIL3). An Arg-Gly-Asp (RGD) motif in the second EGF-like repeat (E2) mediates DEL-1 binding to α_v integrins^{9,10}. Moreover, we have demonstrated that DEL-1 interacts with $\alpha_L\beta_2$ (CD11a/CD18; LFA-1) and $\alpha_M\beta_2$ (CD11b/CD18; Mac-1) integrins^{11,12}. The interaction of DEL-1 with LFA-1 blocks the binding of the latter to its endothelial counter-receptor, intercellular cell adhesion molecule-1 (ICAM-1), thereby inhibiting leukocyte adhesion and recruitment to inflamed sites¹¹.

¹Institute for Clinical Chemistry and Laboratory Medicine, Faculty of Medicine, Technische Universität Dresden, Dresden, Germany. ²National Center for Tumor Diseases, Partner Site Dresden, of the German Cancer Research Center, Heidelberg and of the Faculty of Medicine and University Hospital Carl Gustav Carus, Technische Universität Dresden, Dresden, and of the Helmholtz Association/Helmholtz-Zentrum Dresden-Rossendorf, Dresden, Germany. ³Department of Microbiology, Penn Dental Medicine, University of Pennsylvania, Philadelphia, PA, USA. ⁴Paul Langerhans Institute Dresden, Helmholtz Zentrum München, Faculty of Medicine and University Hospital Carl Gustav Carus, Technische Universität Dresden, Dresden, Germany. ⁵German Center for Diabetes Research, Neuherberg, Germany. ⁶Laboratory of Cytochemistry, Faculty of Biotechnology, University of Wrocław, Wrocław, Poland. ⁷Division of Rheumatology, Medical Clinic III, Faculty of Medicine, Technische Universität Dresden, Dresden, Germany. ⁸Department of Internal Medicine and Radboud Center for Infectious Diseases, Radboud University Medical Center, Nijmegen, The Netherlands. ⁹Oral Immunity and Inflammation Unit, National Institute of Dental and Craniofacial Research, National Institutes of Health, Bethesda, MD, USA. ¹⁰Instituto de Investigaciones Biomédicas (IIBM) 'Alberto Sols', Consejo Superior de Investigaciones Científicas (CSIC) de Madrid, Madrid, Spain. ¹¹Unidad de Biomedicina IIBM-Universidad de las Palmas de Gran Canaria (ULPGC) (Unidad Asociada al CSIC), Instituto Universitario de Investigaciones Biomédicas y Sanitarias, ULPGC, Las Palmas, Spain. ¹²Department of Periodontics, Penn Dental Medicine, University of Pennsylvania, Philadelphia, PA, USA. ¹³These authors contributed equally: Ioannis Kourtzelis, Xiaofei Li. ¹⁴These authors jointly supervised this work: George Hajishengallis, Triantafyllos Chavakis. *e-mail: ioannis.kourtzelis@uniklinikum-dresden.de; geoh@upenn.edu; triantafyllos.chavakis@uniklinikum-dresden.de

By virtue of its anti-inflammatory properties, DEL-1 protects against several inflammation-associated pathologies, such as experimental autoimmune encephalitis/multiple sclerosis¹³, inflammatory bone loss^{9,14}, pulmonary inflammation and fibrosis^{11,15}, and inflammation associated with islet transplantation¹⁶. Proinflammatory cytokines, such as interleukin-17 (IL-17), inhibit endothelial DEL-1 expression, thereby promoting leukocyte infiltration and tissue inflammation^{14,17}. Interestingly, the IL-17-dependent downregulation of DEL-1 is reversed by the pro-resolving lipid mediator resolvin D1 (RvD1), which in turn depends on DEL-1 to mediate protection in a model of inflammatory bone loss¹⁷. The connection of DEL-1 with resolvins raised the possibility that DEL-1 does not simply inhibit the initiation of inflammation but might also promote its resolution, a hypothesis that has not been addressed thus far.

By using two different inflammation models and multiple complementary genetic and pharmacologic approaches, we demonstrate here that DEL-1 contributes to resolution of inflammation by promoting $\alpha_3\beta_3$ integrin-dependent apoptotic neutrophil efferocytosis by macrophages and the emergence of a pro-resolving macrophage phenotype. Consistently, inflammation clearance was correlated with resurgence of DEL-1 expression in humans and mice. DEL-1-dependent efferocytosis triggered a pro-resolving macrophage phenotype in a manner dependent on the liver X receptor (LXR). Importantly, by generating different transgenic mice with cell-specific overexpression of DEL-1, we showed that the cellular source of DEL-1 is a critical determinant of its inflammation-modulatory functions. Specifically, we found that the anti-leukocyte-recruitment action (and hence inhibitory action on initiation of inflammation) was associated with endothelial cell-derived DEL-1, whereas the efferocytic/pro-resolving action was associated with macrophage-derived DEL-1. Therefore, we demonstrate here a new tissue homeostatic concept: the same molecule, DEL-1, not only regulates initiation of inflammation but also promotes inflammation resolution, and this functional versatility is facilitated by its compartmentalized expression. Our present findings on the pro-resolution function of DEL-1 underscore its therapeutic potential against inflammatory diseases.

Results

DEL-1 promotes inflammation resolution in periodontitis. DEL-1 expression is downregulated by inflammation, and humans with inflammatory diseases, including multiple sclerosis and the oral mucosal inflammatory disease periodontitis, express significantly less *EDIL3* messenger RNA (mRNA) in active diseased sites than in inactive or healthy sites^{13,14,18}. Periodontitis, in which neutrophils play a major pathogenic role¹⁹, is a pathology amenable to studies of resolution of inflammation²⁰. Resolution of inflammation in human periodontitis is correlated with reduction in the amount of inflammatory mediators (for example, IL-6 and IL-17) in the fluid exudate adjacent to periodontitis inflamed lesions (gingival crevicular fluid (GCF))²¹. We found that DEL-1 protein levels were significantly elevated in the GCF upon treatment of periodontitis by mechanical debridement (scaling and root planing (SRP)), which leads to clinical inflammatory resolution²², as also confirmed here by assessing probing pocket depth, a parameter that measures inflammatory tissue destruction (Supplementary Fig. 1a). Specifically, DEL-1 protein concentration was compared per patient in GCF samples from a single or multiple sites of periodontal inflammation, before and after clinical inflammatory resolution, and was found to be increased after treatment (Fig. 1). Thus, DEL-1 is upregulated during clearance of human periodontal inflammation. To establish a potential cause-and-effect relationship between DEL-1 and resolution, we used the mouse ligature-induced periodontitis (LIP) model, which has been used extensively to study mechanisms of inflammation and bone loss²³. To study clearance of inflammation, we employed a modified version of the standard LIP model, in which we removed

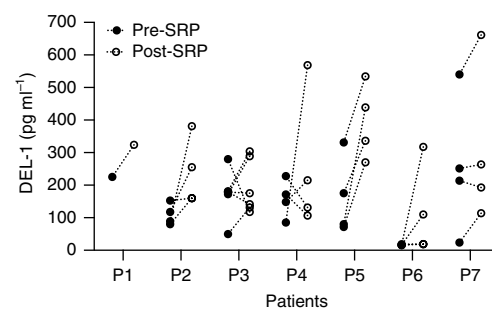


Fig. 1 | DEL-1 concentration is elevated in the GCF following resolution of periodontitis due to treatment with SRP. GCF was collected using PerioPaper strips from distinct periodontitis-involved sites from seven patients (P1–P7) before and after SRP. After elution in 0.1 ml buffer, the GCF was analyzed by ELISA for DEL-1 content. Data represent the concentration of DEL-1 in the eluted GCF samples. $P = 0.0041$ (pre-post paired two-way ANOVA with repeated measures by patient).

the ligature at day 5 and monitored the course of the inflammation for another 5 days. As control, we used mice in which the ligatures were not removed. In wild-type mice, high expression of the proinflammatory cytokine mRNAs *Il6* and *Il17* was induced in the gingival tissue during the initiation phase of inflammation (days 1–5). However, during the resolution phase (days 6–10), *Il6* and *Il17* mRNA expression declined sharply to baseline (Fig. 2a), consistent with the reduction of IL-6 and IL-17 protein in the GCF of periodontitis patients after treatment²¹. Conversely, *Edil3* (hereafter referred to as *Del1*) mRNA and DEL-1 protein (as assessed by specific enzyme-linked immunosorbent assay (ELISA); Supplementary Fig. 1b) declined in concentration during the inflammation initiation phase but were swiftly upregulated in the resolution phase (Fig. 2a,b). Interestingly, the re-emergence of *Del1* in the resolution phase was associated with elevated expression of *Tgfb1* and *Tgfb2*, which are involved in inflammation resolution^{6,24} (Fig. 2a). In wild-type mice in which the ligatures were not removed, the expression of *Del1*, *Tgfb1*, and *Tgfb2* failed to increase after day 5, whereas high expression of *Il6* and *Il17* persisted through day 10 (Fig. 2a).

The removal or not of the ligatures after day 5 defines resolving versus non-resolving inflammation. Consistently, wild-type mice subjected to LIP developed progressive bone loss through day 10, unless the ligatures were removed at day 5, in which case bone loss was arrested (Fig. 2c). Notably, in the same model, DEL-1-deficient (*Del1*^{KO}) mice exhibited persistent bone loss through day 10 even when the ligatures were removed at day 5 (Fig. 2c). In line with their failure to resolve bone loss even when the ligatures were removed, *Del1*^{KO} mice maintained high expression of IL-6 and IL-17 and did not upregulate TGF- β 1 and TGF- β 2 expression, at both the mRNA level (Supplementary Fig. 1c) and the protein level (Fig. 2d), despite ligature removal. Conversely, bone loss arrest upon ligature removal in wild-type litter-mates was correlated with downregulation of IL-6 and IL-17 and upregulation of TGF- β 1 and TGF- β 2 protein and mRNA (Fig. 2d and Supplementary Fig. 1c). Histological analysis of the gingival tissue in the course of LIP and its resolution revealed that neutrophils in *Del1*^{KO} samples were significantly increased compared with wild-type controls, especially in the resolution phase (Supplementary Fig. 1d). To further examine the role of DEL-1 in the regulation of resolution in the LIP model, we determined the concentrations of specialized pro-resolving mediators (SPMs). The amounts of RvD1 and RvE1 were decreased in the GCF from *Del1*^{KO} mice compared with samples from wild-type controls collected 5 days after ligature removal (5DL–5DR; Fig. 2e). Lipoxin A4 was comparable between the two groups (Fig. 2e). Additionally, we tested the ability of exogenous RvD1 administration during

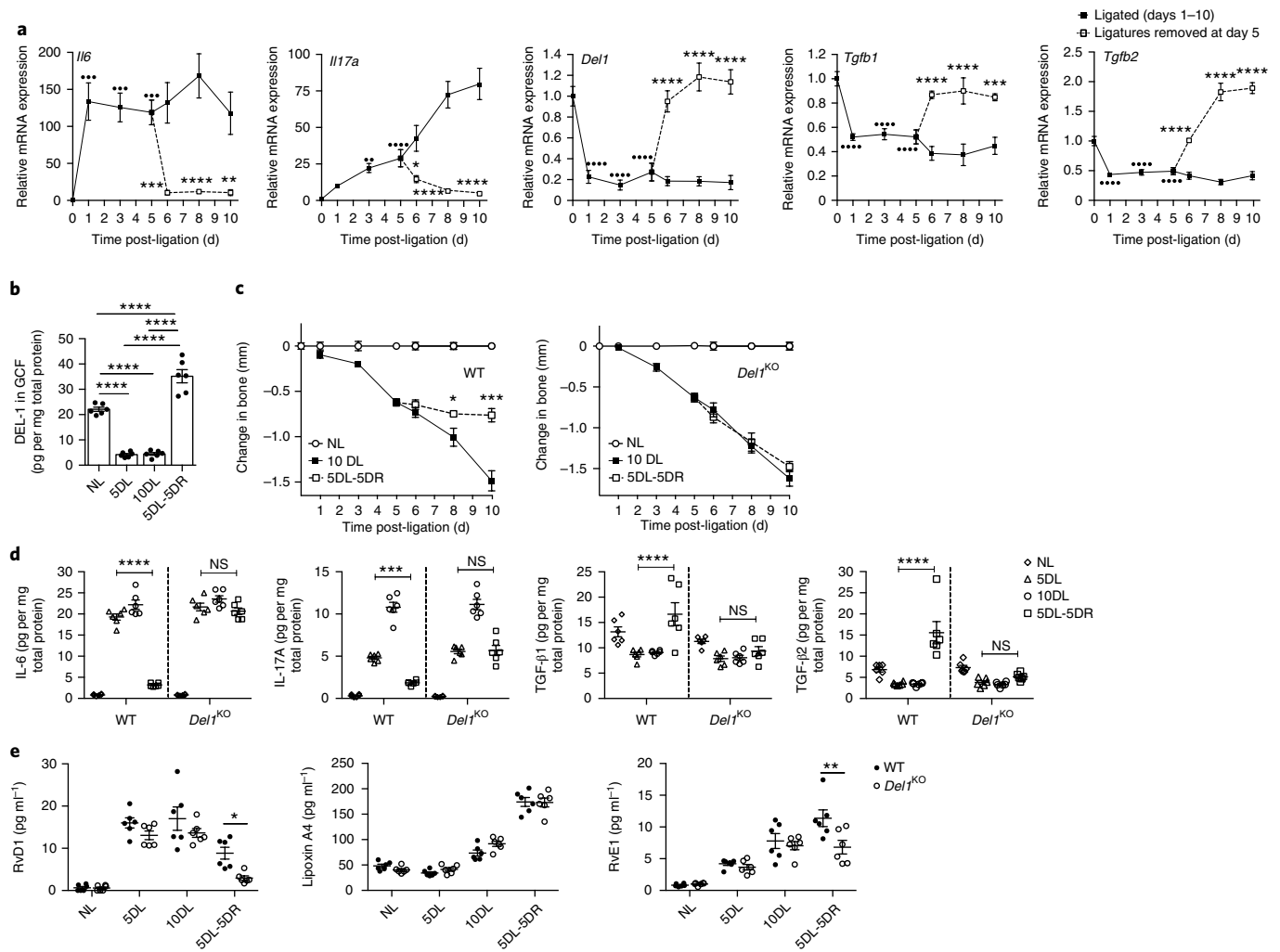


Fig. 2 | The pro-resolution effect of DEL-1 in a resolving model of mouse LIP. **a**, Wild-type (WT) mice were subjected to LIP for up to 10 days, and ligatures were removed or not at day 5 ($n=5$ mice per group per time point). Relative mRNA expression of the indicated molecules in gingival tissue was assayed by real-time PCR. Data were normalized to *Gapdh* mRNA and are presented as fold change relative to baseline, set as 1. **b**, WT mice were subjected to LIP for up to 10 days, and ligatures were removed or not at day 5 ($n=6$ mice per group per time point). Protein concentration of DEL-1 was measured by ELISA in GCF that was recovered from ligatures. **c**, Bone loss was measured in litter-mate WT or *Del1*^{KO} mice that were subjected to LIP for up to 10 days with or without ligature removal at day 5 ($n=5$ mice per group). **d,e**, WT or *Del1*^{KO} litter-mate mice were subjected to LIP for up to 10 days, and ligatures were removed or not at day 5 ($n=6$ mice per group). **d**, Protein concentrations of IL-6, IL-17A, TGF- β 1, and TGF- β 2 were assessed in gingival tissue by ELISA. **e**, Concentrations of RvD1, lipoxin A4, and RvE1 were measured in GCF recovered from ligatures. $**P < 0.01$, $***P < 0.001$, $****P < 0.0001$ versus day 0 (baseline) (**a**); $*P < 0.05$, $**P < 0.01$, $***P < 0.001$, $****P < 0.0001$ versus corresponding time point without ligature removal (**a** and **c**) or between indicated groups (**b,d,e**). Statistical tests were as follows: one-way ANOVA with Dunnett's multiple comparisons test for comparison with baseline and two-way ANOVA with Sidak's multiple comparisons test for comparisons with corresponding time point without ligature removal (**a**); one-way ANOVA with Tukey's multiple comparisons test (**b**); two-tailed Student's *t*-test (**c**); two-way ANOVA and Tukey's multiple comparisons test (**d,e**). Data are presented as mean \pm s.e.m. and are derived from one experiment with independent mice at each time point (**a,c**) or pooled from two experiments (**b,d,e**). NL, not ligated; 5DL, 5 days ligated; 10DL, 10 days ligated; 5DL-5DR, 5 days ligated and 5 days with ligatures removed; NS, non-significant.

the resolution phase of LIP to promote inflammation resolution in DEL-1 deficiency. Whereas exogenously added RvD1 further promoted inflammation resolution in wild-type mice, it failed to promote resolution in *Del1*^{KO} mice (Supplementary Fig. 1e–g). Taken together, these findings indicate that DEL-1 deficiency is associated with defective resolution of inflammation.

DEL-1 clears inflammation through efferocytosis. We next investigated mechanisms of DEL-1 involvement in inflammation resolution. To obtain mechanistic insights and to investigate whether the observed action of DEL-1 represents a more general principle in resolution of inflammation, we engaged established models of

peritoneal inflammation and resolution^{25–27}. Analysis of the peritoneal exudate (Supplementary Fig. 2a) following monosodium urate (MSU) crystal injection revealed higher neutrophil numbers in *Del1*^{KO} mice compared with wild-type controls (Fig. 3a–c). DEL-1 deficiency also enhanced monocyte/macrophage recruitment only at the 8 h time point (Supplementary Fig. 2b). Given our previous reports that DEL-1 can inhibit both $\alpha_L\beta_2$ and $\alpha_M\beta_2$ integrins on leukocytes^{11,12}, we first studied the involvement of these recruitment receptors in initiation of MSU-induced inflammation. On the one hand, absence of $\alpha_L\beta_2$ integrin resulted in decreased neutrophil recruitment at 8 h (Supplementary Fig. 2c), whereas the infiltration of monocytes/macrophages remained unaffected (Supplementary

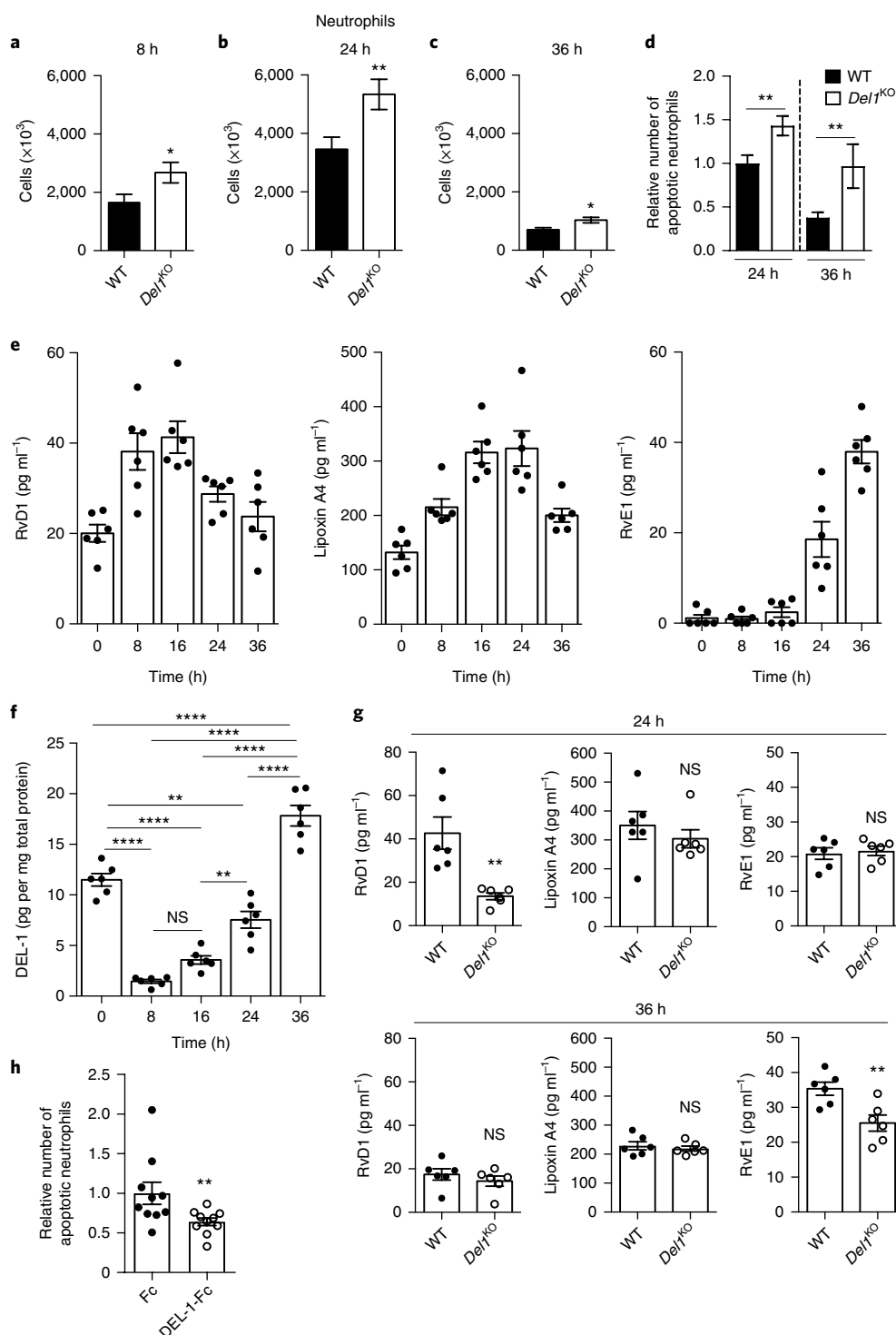


Fig. 3 | DEL-1 modulates resolution of acute inflammation. **a–c**, Numbers of neutrophils in peritoneal exudates obtained from *Del1^{KO}* and their respective WT mice at 8 h (**a**; $n = 11$ WT and 13 *Del1^{KO}* mice), 24 h (**b**; $n = 18$ WT and 16 *Del1^{KO}* mice), and 36 h (**c**; $n = 8$ mice per group) after MSU crystal-induced inflammation. **d**, Relative number of apoptotic neutrophils detected in peritoneal exudates 24 and 36 h after MSU crystal injection in WT or *Del1^{KO}* mice. Number of apoptotic neutrophils was measured and expressed relative to the WT 24 h group, set as 1 (24 h, $n = 18$ WT and 16 *Del1^{KO}* mice; 36 h, $n = 8$ mice per group). **e, f**, Concentrations of RvD1, lipoxin A4, and RvE1 (**e**) and protein concentration of DEL-1 (pg per mg total protein) (**f**) were measured in the supernatant of peritoneal fluid obtained from untreated (0 h) WT mice or WT mice at 8, 16, 24, and 36 h after MSU crystal-induced inflammation ($n = 6$ mice per group). **g**, Concentrations of RvD1, lipoxin A4, and RvE1 were measured in the supernatant of peritoneal exudates obtained from WT or *Del1^{KO}* mice at 24 and 36 h after MSU crystal-induced inflammation ($n = 6$ mice per group). **h**, MSU crystals were injected in WT mice and, after 20 h, 5 μ g of DEL-1-Fc or Fc control protein were administered intraperitoneally; 4 h after the latter injection, the relative number of apoptotic neutrophils in peritoneal exudates was assessed. Numbers of apoptotic neutrophils are expressed relative to the Fc control group, set as 1 ($n = 10$ mice per group). * $P < 0.05$, ** $P < 0.01$, **** $P < 0.0001$, NS, non-significant. Statistical tests were as follows: two-tailed Student's *t*-test (**a, b**); two-tailed Mann-Whitney *U*-test (**c, d, g, h**); one-way ANOVA with Tukey's multiple comparisons test (**f**). Data are presented as mean \pm s.e.m. and are pooled from two experiments (**a, c, d**, 36 h time point; **e–h**) or three experiments (**b, d**, 24 h time point).

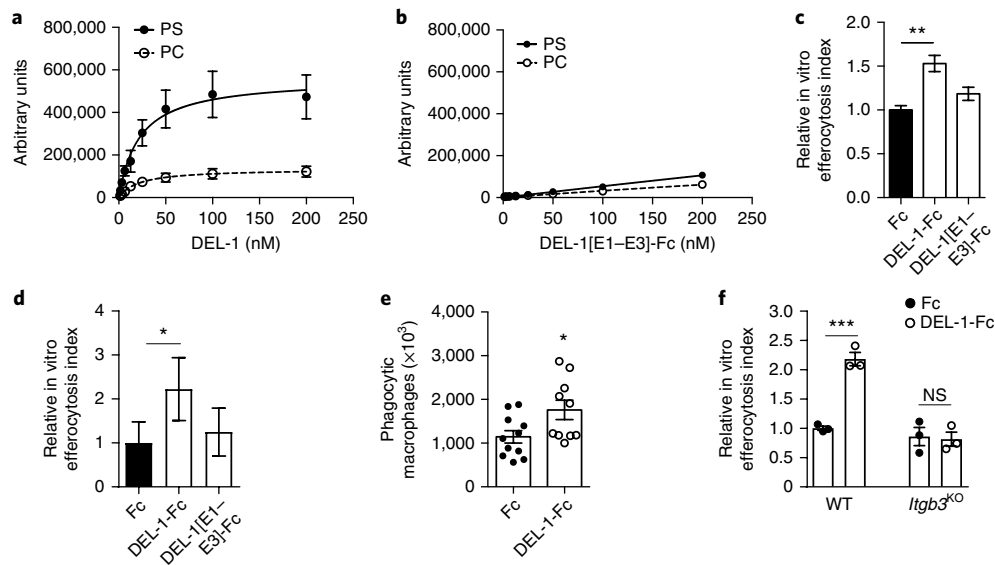


Fig. 4 | DEL-1 enhances efferocytosis activity through interaction with phosphatidylserine and $\alpha_5\beta_1$ integrin. **a,b**, Saturation binding of full-length DEL-1 (**a**) or DEL-1 protein that lacks the discoidin I-like domains expressed as an Fc fusion protein (DEL-1[E1-E3]-Fc; **b**) to liposomes composed of PC/Chol (PC) or PC/Chol/PS (PS) ($n=3$ preparations in **a** and $n=2$ preparations in **b**). **c,d**, Primary BMDMs from WT mice ($n=3$ separate cell isolations; **c**) or human MDMs ($n=5$ separate cell isolations; **d**) were co-cultured for 30 min with apoptotic neutrophils (mouse or human, respectively) that were pre-stained with BCECF acetoxymethyl ester in the presence of Fc control, full-length DEL-1-Fc, or DEL-1 protein lacking the discoidin I-like domains (DEL-1[E1-E3]-Fc) (each 500 ng ml^{-1}). Relative efferocytosis index is shown and was calculated as the ratio of the number of macrophages that have phagocytosed apoptotic material to the total number of macrophages. Data are expressed relative to the Fc control group, set as 1. **e**, WT mice were injected intraperitoneally with thioglycolate, and 72 h thereafter they received a second intraperitoneal injection of 5×10^6 pre-stained apoptotic neutrophils together with $5 \mu\text{g}$ of either Fc control or DEL-1-Fc; 3 h after the latter injection, mice were killed, and the number of phagocytic macrophages was analyzed ($n=11$ mice for Fc control and 10 mice for DEL-1-Fc). **f**, In vitro phagocytosis assay was performed as described in **c**. Relative efferocytosis index of BMDMs from mice deficient in β_3 integrin (*Itgb3*^{KO}) and of BMDMs from respective control mice (WT) in the presence of Fc control or DEL-1-Fc is shown ($n=3$ separate cell isolations per genotype). * $P < 0.05$, ** $P < 0.01$, *** $P < 0.001$, NS, non-significant. Statistical tests are as follows: one-way ANOVA with Dunnett's (**c,d**) or Tukey's (**f**) multiple comparisons test; two-tailed Student's *t*-test (**e**). Data are presented as mean \pm s.e.m. and are derived from three experiments (**a**), from two experiments (**b,e**), or from one experiment (**c,f**) or are pooled from five experiments (**d**).

Fig. 2d). On the other hand, antibody blockade of $\alpha_M\beta_2$ integrin led to decreased neutrophil (Supplementary Fig. 2e) and monocyte/macrophage (Supplementary Fig. 2f) accumulation at the 8 h time point. Thus, DEL-1 likely inhibits initial $\alpha_1\beta_2$ - and $\alpha_M\beta_2$ -dependent recruitment of neutrophils and $\alpha_M\beta_2$ -dependent recruitment of monocytes in MSU crystal-induced inflammation.

To address the role of DEL-1 in inflammation clearance in this model, we determined the abundance of apoptotic neutrophils at 24 and 36 h post-MSU injection. We found increased numbers of apoptotic neutrophils in *Del1*^{KO} mice compared with wild-type mice (Fig. 3d), which might be attributed to non-redundant DEL-1-mediated regulation of apoptotic cell clearance. Given the importance of SPMs in mediating inflammation resolution²⁸, we next performed kinetic analysis of SPMs and DEL-1 in the supernatant of peritoneal exudates in the course of MSU crystal-induced inflammation (Fig. 3e,f). The kinetic SPM data in the MSU peritonitis model (Fig. 3e) were comparable to previous SPM kinetic analyses in acute self-limited inflammation^{29–31}. Consistent with findings from the LIP model, in the course of MSU crystal-induced inflammation, RvE1 followed a similar pattern to that of DEL-1; the concentrations of both molecules in the peritoneal exudate progressively increased from the 16 h time point onwards (Fig. 3e,f). To further investigate the pro-resolving role of DEL-1, SPM concentrations were assessed in peritoneal exudates from wild-type and *Del1*^{KO} mice collected during inflammation resolution. Notably, and in line with findings from the LIP model, DEL-1 deficiency resulted in decreased concentrations of RvD1 and RvE1 at 24 and 36 h post-MSU injection, respectively (Fig. 3g). Conversely, expression

analysis of *Gpr18*, *Chemr23*, and *Fpr2*, which encode SPM receptors, in peritoneal monocytes/macrophages sorted 24 h after MSU crystal-induced inflammation revealed comparable expression between wild-type and *Del1*^{KO} mice (Supplementary Fig. 2g).

To assess whether DEL-1 is a non-redundant effector of SPMs, we examined the effect of exogenous RvD1 administration on inflammation resolution in the presence or absence of endogenous DEL-1 using the MSU crystal-induced inflammation model. Simultaneous administration of RvD1 and MSU crystals led to enhanced clearance of apoptotic neutrophils in wild-type but not in *Del1*^{KO} mice 24 h after induction of inflammation (Supplementary Fig. 2h). The failure of RvD1 to restore defective clearance of apoptotic neutrophils in *Del1*^{KO} mice suggests that DEL-1 mediates at least part of the SPM-dependent pro-resolution program.

To further confirm the pro-resolving function of DEL-1, we administered soluble recombinant DEL-1 (expressed as an Fc fusion protein, DEL-1-Fc) 20 h after treatment with MSU crystals (that is, after a large portion of neutrophil recruitment has already taken place^{26,27}) and analyzed the cellular exudate 4 h thereafter. Treatment with DEL-1-Fc reduced numbers of apoptotic neutrophils in the exudate compared with treatment with Fc control protein (Fig. 3h), suggesting that DEL-1 enhances the clearance of apoptotic neutrophils.

We therefore set out to understand the mechanism whereby DEL-1 enhances the phagocytosis of apoptotic neutrophils by macrophages. At its C terminus, DEL-1 has two discoidin I-like domains that are involved in the binding of phospholipid moieties³². Consistent with this property, DEL-1 bound with high affinity (dissociation constant $K_d \approx 26 \text{ nM}$) to liposomes containing PS (Fig. 4a),

a major 'eat-me' signal on the surface of apoptotic cells. The binding of DEL-1 to PS was attributed to the discoidin I-like domains, since a truncated version of DEL-1 lacking these domains (DEL-1[E1–E3]-Fc) failed to interact with PS (Fig. 4b). Accordingly, DEL-1-Fc but not DEL-1[E1–E3]-Fc or Fc control protein promoted efferocytosis of apoptotic neutrophils by macrophages in vitro in both the mouse and human systems (Fig. 4c,d).

To further establish the role of DEL-1-Fc in promoting efferocytosis using an independent in vivo model, we performed thioglycolate-induced peritonitis, which is conducive for studying specific aspects of efferocytosis. Specifically, wild-type mice were injected intraperitoneally with thioglycolate and after 72 h, when the peritoneal exudate has few neutrophils³³, they received a second intraperitoneal injection of 5×10^6 fluorescently pre-stained (with 2',7'-bis(2-carboxyethyl)-5,6-carboxyfluorescein (BCECF)) apoptotic neutrophils together with DEL-1-Fc or Fc control. Mice were killed 3 h later, and the numbers of efferocytic (BCECF⁺F4/80⁺) macrophages in the peritoneal exudate were determined by flow cytometry. Treatment with DEL-1-Fc significantly increased numbers of efferocytic macrophages compared with treatment with Fc control protein (Fig. 4e).

To address which of the two DEL-1 receptors on macrophages that are involved in macrophage efferocytosis^{10,12,34,35}, $\alpha_v\beta_3$ integrin and $\alpha_M\beta_2$ integrin, was the receptor mediating the DEL-1-dependent efferocytic activity, we engaged macrophages from β_3 integrin- and α_M integrin-deficient mice. DEL-1-Fc failed to promote efferocytosis of apoptotic neutrophils by β_3 integrin-deficient macrophages (Fig. 4f). However, DEL-1-Fc significantly enhanced efferocytosis of apoptotic neutrophils by α_M integrin-deficient macrophages (data not shown). Taken together, these findings indicate that DEL-1 enhances resolution of peritoneal inflammation by promoting $\alpha_v\beta_3$ integrin-mediated efferocytosis.

DEL-1 triggers a pro-resolving macrophage phenotype. We next investigated the consequences of DEL-1-mediated clearance of apoptotic neutrophils on the efferocytic macrophages. Wild-type and *Del1*^{KO} mice were subjected to MSU crystal-induced peritoneal inflammation for 24 h (a time point by which significant efferocytosis occurs), and monocytes/macrophages were then sorted and analyzed for the expression of genes serving as markers of the resolving macrophage phenotype^{7,36}. We found that DEL-1 deficiency caused reduction in the expression of genes encoding TGF- β 1; the nuclear receptors/transcription factors LXR α and LXR β ; retinoid X receptor α (RXR α); ATP-binding cassette transporter 1 (ABCA1) and transglutaminase 2 (TGM2), which are molecules downstream of LXR signaling; and the efferocytosis-associated molecules AXL, CD36, and uncoupling protein 2 (UCP2) (Fig. 5a). Importantly, the absence of DEL-1 had no effect on the expression of factors associated with the resolving macrophage phenotype at steady state (Supplementary Fig. 3a), suggesting that DEL-1 regulates these factors only in the context of inflammation resolution.

In further in vitro experiments, we studied the role of DEL-1-dependent efferocytosis in the expression of factors associated with resolution of inflammation. Addition of DEL-1-Fc to efferocytosis cultures (macrophages, either bone marrow-derived macrophages (BMDMs) or isolated peritoneal macrophages, incubated with apoptotic neutrophils) stimulated the upregulation of TGF- β 1 protein secretion in the cultures (Fig. 5b,c). Moreover, DEL-1-Fc enhanced mRNA expression of *Tgfb1* and additional markers of resolution (*Lxra*, *Lxrb*, *Ucp2*, *Abca1*, *Tgm2*, and *Rxra*) in macrophages from the efferocytosis cultures (Supplementary Fig. 3b–i). Macrophages treated with DEL-1-Fc in the absence of apoptotic neutrophils did not demonstrate any phenotypic alterations (Supplementary Fig. 3j), confirming that these upregulatory effects of DEL-1 are exerted only in the context of efferocytosis. Both the point mutant DEL-1[RGE]-Fc, which lacks the functional RGD motif and hence

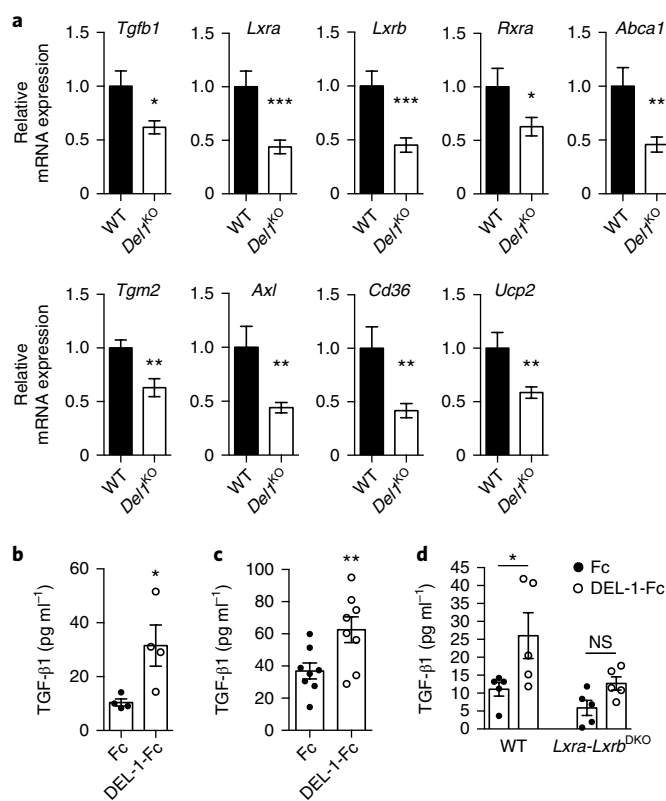


Fig. 5 | DEL-1 promotes phenotypic alterations in macrophages during inflammation resolution through LXR.

a, Relative mRNA expression of *Tgfb1*, *Lxra*, *Lxrb*, *Rxra*, *Abca1*, *Tgm2*, *Axl*, *Cd36*, and *Ucp2* in peritoneal monocytes/macrophages sorted from *Del1*^{KO} mice and their WT littermates 24 h after MSU crystal-induced inflammation. Relative mRNA expression was normalized against 18S rRNA and was set as 1 in WT monocytes/macrophages ($n = 7$ WT and 12 *Del1*^{KO} mice). **b,c**, Protein concentrations of TGF- β 1 were measured in efferocytosis culture supernatants of BMDMs ($n = 4$ separate cell isolations; **b**) or isolated peritoneal macrophages ($n = 8$ separate cell isolations; **c**) incubated for 3 h with mouse apoptotic neutrophils in the presence of Fc control or DEL-1-Fc (500 ng ml⁻¹ each). **d**, Protein concentrations of TGF- β 1 in the supernatants of co-cultures of apoptotic neutrophils with BMDMs from mice deficient in both LXR α and LXR β (*Lxra-Lxrb*^{DKO}) or BMDMs from their respective control mice (WT) incubated for 3 h in the presence of Fc control or DEL-1-Fc (each 500 ng ml⁻¹) ($n = 5$ separate cell isolations per genotype). * $P < 0.05$, ** $P < 0.01$, *** $P < 0.001$, NS, non-significant. Statistical tests are as follows: two-tailed Student's *t*-test (**a,b,c**); one-way ANOVA with Tukey's multiple comparisons test (**d**). Data are presented as mean \pm s.e.m. and are pooled from two experiments (**a,c**), are from one experiment representative of two experiments (**b**), or are from one experiment (**d**).

does not interact with the $\alpha_v\beta_3$ integrin, and the truncated protein DEL-1[E1–E3]-Fc, which lacks the discoidin I-like domains and does not bind PS, failed to induce the resolving phenotype in macrophages (Supplementary Fig. 4a–c), thus confirming that the pro-resolving effects of DEL-1 require its concomitant interactions with β_3 integrin and PS. Inactivation of β_3 integrin conclusively demonstrated that this integrin is required for the DEL-1-mediated switch of efferocytic macrophages towards a resolving phenotype (Supplementary Fig. 4d).

The in vivo and ex vivo experiments described thus far showed that DEL-1 regulates the expression of *Lxra*, *Lxrb*, and their downstream effector *Tgm2*, which enhances the efferocytic activity of macrophages³⁷. We therefore determined the role of LXRs as

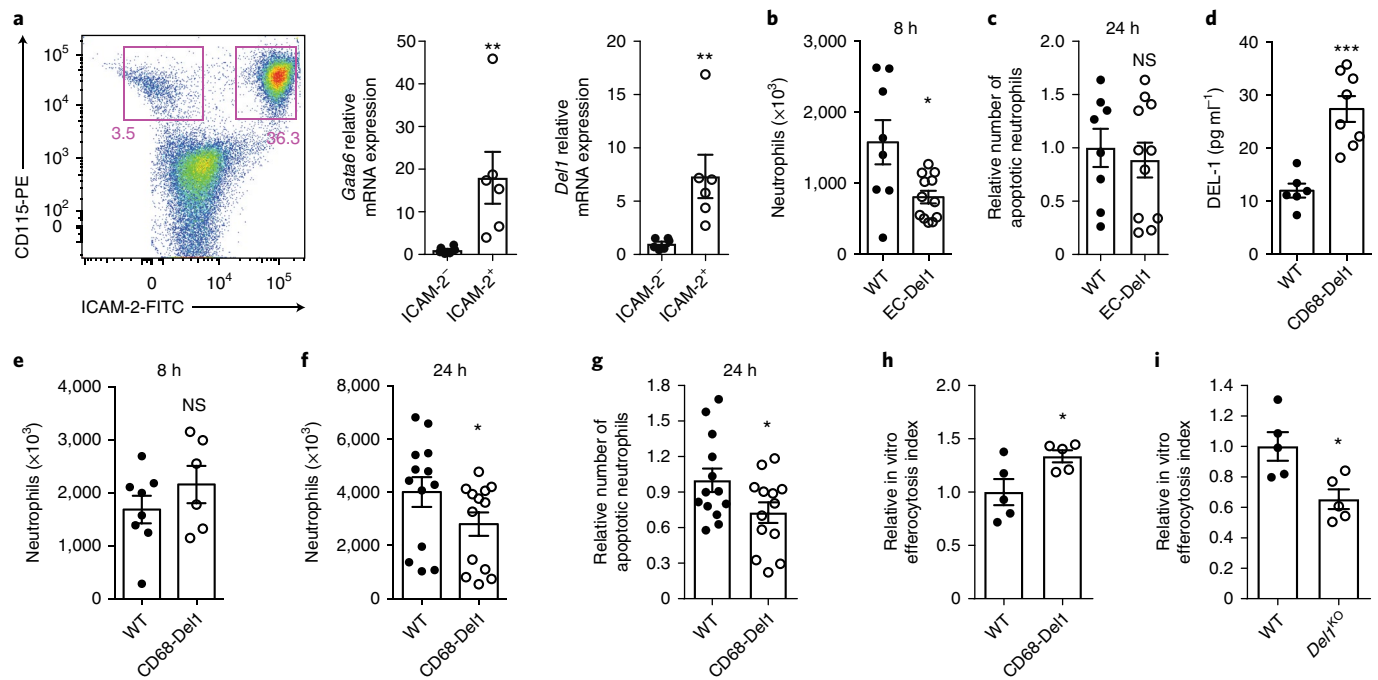


Fig. 6 | Compartmentalized expression of DEL-1 regulates resolution of acute inflammation. **a**, Representative fluorescence-activated cell sorting plot and relative mRNA expression of *Gata6* and *Del1* in CD115⁺ICAM-2⁻ macrophages and CD115⁺ICAM-2⁺ resident macrophages sorted from peritoneum of WT mice at steady state ($n = 6$ mice). Numbers in outlined areas (far left plot) indicate percent CD115⁺ICAM-2⁻ macrophages (left) or CD115⁺ICAM-2⁺ macrophages (right). Relative mRNA expression was normalized against 18S rRNA and was set as 1 in CD115⁺ICAM-2⁻ macrophages. **b**, Neutrophil numbers in peritoneal exudates collected 8 h after MSU crystal injection in mice overexpressing DEL-1 in the endothelium (EC-Del1 mice) or their WT litter-mates ($n = 8$ WT and 12 EC-Del1 mice). **c**, Relative number of apoptotic neutrophils detected in peritoneal exudates 24 h after MSU crystal injection in WT litter-mate or EC-Del1 mice. Number of apoptotic neutrophils was measured and expressed relative to the WT group, set as 1 ($n = 8$ WT and 11 EC-Del1 mice). **d**, DEL-1 protein concentration in the supernatant of isolated peritoneal macrophages derived from untreated (not subjected to MSU crystal-induced inflammation) mice that overexpress DEL-1 under control of the CD68 promoter (CD68-Del1) or their WT litter-mates ($n = 6$ separate cell isolations for WT mice and 8 for CD68-Del1 mice). **e, f**, Numbers of neutrophils in peritoneal exudates obtained from CD68-Del1 mice or their WT litter-mates at 8 h (**e**) and 24 h (**f**) after MSU crystal-induced inflammation ($n = 8$ WT and 6 CD68-Del1 mice in **e** and $n = 13$ mice per group in **f**). **g**, Relative numbers of apoptotic neutrophils in peritoneal exudates obtained from WT and CD68-Del1 mice 24 h after MSU crystal-induced inflammation. Numbers of apoptotic neutrophils are expressed relative to the WT group, set as 1 ($n = 13$ mice per group). **h, i**, Isolated peritoneal macrophages from untreated CD68-Del1 mice (**h**) or untreated *Del1*^{KO} mice (**i**) and from the respective untreated WT mice were incubated for 30 min with apoptotic neutrophils that were pre-stained with BCECF acetoxymethyl ester. Relative efferocytosis index is shown and was calculated as the ratio of the number of macrophages that have phagocytosed apoptotic material to the total number of macrophages. Data are expressed relative to the respective WT group, set as 1 ($n = 5$ separate cell isolations per genotype). * $P < 0.05$, ** $P < 0.01$, *** $P < 0.001$, NS, non-significant. Statistical tests are as follows: two-tailed Student's *t*-test (**b, c, g**); two-tailed Mann-Whitney *U*-test (**a, d, e, f, h, i**). Data are presented as mean \pm s.e.m. and are from one experiment representative of two (**a**) or are pooled from two experiments (**b–g**) or from three experiments (**h, i**).

possible mediators of the DEL-1-dependent resolving macrophage phenotype. Genetic deficiency of both *Lxra* and *Lxrb* or treatment of macrophages with an LXR antagonist significantly attenuated the DEL-1-dependent upregulation of TGF- β 1 in macrophages from efferocytosis cultures (Fig. 5d and Supplementary Fig. 4e) but did not affect *Tgfb1* expression in macrophages that were not exposed to apoptotic neutrophils (Supplementary Fig. 4f, g). In conclusion, DEL-1 promotes a resolving phenotype in macrophages by enhancing efferocytosis and production of pro-resolving markers in a manner that is—at least in part—dependent on LXR signaling.

DEL-1 localization determines its pro-resolving activity. The anti-leukocyte-recruitment activity of DEL-1 was assumed to be mediated by endothelial cell-secreted DEL-1^{11,14}. In the present study, although DEL-1 deficiency resulted in defective resolution, the endogenous cellular source of DEL-1 promoting efferocytosis in wild-type mice was uncertain. We thus next investigated the cellular sources of DEL-1 predominantly involved in these distinct functions under the hypothesis that macrophage-derived DEL-1 regulates efferocytosis, whereas endothelial cell-derived DEL-1 regulates

leukocyte recruitment. Interestingly, DEL-1 expression was previously identified in resident macrophages, and *Del1* was identified as a gene selective for peritoneal-resident macrophages^{38,39}. We verified that *Del1* was expressed by resident peritoneal macrophages, and, in particular, by GATA-6⁺ macrophages (Fig. 6a), which were previously ascribed an essential role in acute inflammation resolution³⁹.

We next assessed whether the two distinct functions of DEL-1, inhibition of leukocyte recruitment and promotion of efferocytosis, are correlated with its spatial cellular distribution in endothelial cells and macrophages, respectively. Using mice with endothelial-specific overexpression of DEL-1 (EC-Del1) in the acute MSU crystal-induced inflammation model, we found that neutrophil recruitment during the initial phase of MSU crystal-induced inflammation was significantly decreased in peritoneal exudates from EC-Del1 mice compared with litter-mate controls (Fig. 6b). In contrast, endothelial-specific DEL-1 overexpression failed to promote the clearance of apoptotic neutrophils assessed at 24 h post-MSU injection (Fig. 6c). Conversely, in the same assays, mice with macrophage-specific DEL-1 overexpression (under control of the CD68 promoter; Fig. 6d and Supplementary Fig. 5a) did not display any difference

in initial neutrophil recruitment (Fig. 6e) but demonstrated a significant decrease in numbers of total neutrophils and apoptotic neutrophils at 24 h (Fig. 6f,g). The impact of macrophage-specific overexpression of DEL-1 on inflammation resolution was corroborated using our *in vitro* efferocytosis assay. DEL-1-overexpressing peritoneal macrophages exhibited enhanced efferocytosis compared with wild-type cells (Fig. 6h). Conversely, but consistently, peritoneal macrophages from *Del1*^{KO} mice exhibited a decreased efferocytosis index compared with macrophages derived from wild-type controls (Fig. 6i). Macrophage-specific overexpression of truncated DEL-1 that lacks the discoidin I-like domains (DEL-1[E1–E3]; Supplementary Fig. 5b) in mice failed to influence the numbers of total neutrophils and of apoptotic neutrophils, compared with their respective wild-type controls (Supplementary Fig. 5c,d), confirming the specificity of the overexpression effect and the requirement for PS binding.

Having shown the importance of macrophage $\alpha_v\beta_3$ integrin in DEL-1-dependent efferocytosis, we next examined whether macrophage-derived DEL-1 might interfere with additional receptor pairs potentially involved in the formation of the phagocytic synapse. To this end, we performed *in vitro* efferocytosis assays with macrophages overexpressing full-length DEL-1, in the presence or absence of antibody-mediated inhibition of the receptors LFA-1 and Mac-1 or their counter-receptor ICAM-1. None of the tested inhibitors influenced DEL-1-dependent efferocytosis (Supplementary Fig. 6a,b). Together, these data unveil that the efferocytosis and inflammation resolution functions are primarily associated with macrophage-derived DEL-1, whereas endothelial-derived DEL-1 is primarily involved in restraining leukocyte recruitment and initiation of inflammation.

Discussion

Inflammation resolution does not represent passive termination of inflammatory responses but rather a well-coordinated active process to reinstate tissue integrity and function^{1,2}. Although SPMs play important roles in resolution²⁸, the network of molecules and mechanisms that coordinate this complex process is incompletely understood. DEL-1 was previously implicated as an inhibitor of inflammatory cell recruitment and initiation of inflammation^{11,14,16}. We now demonstrate that DEL-1 pro-actively modulates inflammation resolution by facilitating efferocytosis and by inducing phenotypic alterations in macrophages, driving them towards a resolving phenotype. Moreover, the present study indicates that DEL-1 is a non-redundant effector of SPM-dependent inflammation resolution and is required for optimal production of at least certain important SPMs (RvD1 and RvE1). Our findings, therefore, establish DEL-1 as an endogenous regulator of functional immune plasticity.

In line with its upregulation during resolution of human or experimental mouse periodontitis, DEL-1 had a non-redundant pro-resolving role in two mouse inflammatory models. First, DEL-1 deficiency resulted in non-resolving inflammation and persistent bone loss, associated with reduced amounts of RvD1 and RvE1, in a modified model of LIP that allowed the study of inflammation resolution. These findings are therapeutically important for periodontitis, an oral inflammatory disease associated with increased risk for systemic disorders⁴⁰.

To determine whether the pro-resolving action of DEL-1 in periodontitis can be generalized to different settings and to elucidate potential mechanisms of inflammation resolution involving DEL-1, we employed a model of self-limited MSU crystal-induced peritoneal inflammation. In this model, endogenous DEL-1 deficiency caused defective clearance of apoptotic neutrophils and attenuated expression of resolving markers in macrophages; conversely, administration of exogenous DEL-1 resulted in improved inflammation resolution. In terms of structure–function relationships, we showed that DEL-1 binds to PS through its discoidin I-like domains, thereby

enabling the recognition of apoptotic neutrophils. Moreover, the additional interaction of DEL-1 with $\alpha_v\beta_3$ integrin on macrophages through the RGD site in its second EGF-like repeat promotes the uptake of apoptotic neutrophils.

Intriguingly, the pro-resolving effect of exogenously added RvD1 failed in *Del1*^{KO} mice, and furthermore, the defective efferocytosis in *Del1*^{KO} mice resulted in decreased production of endogenous SPMs, an effect that would further aggravate defective resolution associated with DEL-1 deficiency. Thus, DEL-1 not only is an essential effector of inflammation resolution but also promotes SPM production, therefore possibly generating a positive-feedback loop that reinforces resolution. These mechanistic findings reveal a new connection between DEL-1 and resolvins and might in part explain the successful use of resolvins in preclinical models of inflammatory diseases^{41,42}.

The nuclear receptor LXR regulates important aspects of immunity and inflammation^{43,44}. The ability of DEL-1 to upregulate TGF- β 1 in efferocytic macrophages was, at least in part, dependent on *Lxra* and *Lxrb*. Moreover, DEL-1 upregulated both LXR isoforms and dependent downstream molecules, such as TGM2, which enhances apoptotic cell clearance by macrophages³⁷, suggesting that DEL-1 promotes LXR activation. In this regard, given its lipid-binding capacity, DEL-1 might increase the local concentration or availability of lipid agonists derived from engulfed apoptotic material, thereby promoting LXR activation in efferocytic macrophages^{43,45}. LXR activation in macrophages was also shown to inhibit lipopolysaccharide-induced expression of cytokines such as IL-1 β and IL-6⁴⁶ that contribute to induction of the T_H17 subset of helper T cells. This mechanism might in part explain the persistence of the gingival IL-17 response in *Del1*^{KO} mice despite ligature removal, which in DEL-1-proficient mice leads to resolution. IL-17 has been implicated as the driver of destructive inflammation associated with DEL-1 deficiency in preclinical models of periodontitis and multiple sclerosis^{13,14}.

DEL-1 associates with the cell surface and extracellular matrix and is a highly adhesive protein, which might substantially prevent its diffusion upon secretion^{11,47}. Therefore, the expression of DEL-1 at a site where it is specifically needed becomes a critical regulatory issue for homeostatic immunity. This notion is consistent with our experimental evidence herein showing that mice overexpressing DEL-1 in their endothelium displayed decreased neutrophil recruitment upon MSU crystal-induced inflammation while maintaining unaltered efferocytic/pro-resolving activity. The latter activity was enhanced by macrophage-specific overexpression of DEL-1, lending support to this location-dependent homeostatic principle. This location principle might constitute a critical determinant of the immunomodulatory functions of additional homeostatic molecules. A future study using mice with a conditional *Del1* allele and a myeloid cell-specific deletion of DEL-1 could fully address the physiological relevance of the pro-resolving action of macrophage-derived DEL-1.

We additionally confirmed here that *Del1* was predominantly expressed by GATA-6⁺ macrophages^{38,39}, which represent resident macrophages. This finding, together with the local endothelial expression of DEL-1, is consistent with the emerging understanding that local tissues are not passive recipients of recruited immune surveillance but rather have a regulatory ‘say’ over inflammatory responses^{8,48,49}.

Taken together, our present findings support that the versatile functionality of DEL-1 is dependent upon distinct structural domains and the differential spatiotemporal expression of this molecule. DEL-1 is a determinant of functional immune plasticity at the tissue level and has a dual mode of action in the course of inflammation. It can both regulate inflammatory cell recruitment and shape macrophage plasticity towards a resolving phenotype, each of which could be therapeutically exploited to inhibit destructive

inflammation and mediate the reconstitution of tissue integrity in inflammatory diseases.

Online content

Any methods, additional references, Nature Research reporting summaries, source data, statements of data availability and associated accession codes are available at <https://doi.org/10.1038/s41590-018-0249-1>.

Received: 5 February 2018; Accepted: 26 September 2018;
Published online: 19 November 2018

References

- Fullerton, J. N. & Gilroy, D. W. Resolution of inflammation: a new therapeutic frontier. *Nat. Rev. Drug. Discov.* **15**, 551–567 (2016).
- Serhan, C. N. Pro-resolving lipid mediators are leads for resolution physiology. *Nature* **510**, 92–101 (2014).
- Serhan, C. N., Chiang, N. & Dalli, J. The resolution code of acute inflammation: novel pro-resolving lipid mediators in resolution. *Semin. Immunol.* **27**, 200–215 (2015).
- Greenlee-Wacker, M. C. Clearance of apoptotic neutrophils and resolution of inflammation. *Immunol. Rev.* **273**, 357–370 (2016).
- Birge, R. B. et al. Phosphatidylserine is a global immunosuppressive signal in efferocytosis, infectious disease, and cancer. *Cell Death Differ.* **23**, 962–978 (2016).
- Ortega-Gómez, A., Perretti, M. & Soehnlein, O. Resolution of inflammation: an integrated view. *EMBO Mol. Med.* **5**, 661–674 (2013).
- A-Gonzalez, N. & Hidalgo, A. Nuclear receptors and clearance of apoptotic cells: stimulating the macrophage's appetite. *Front. Immunol.* **5**, 211 (2014).
- Hajishengallis, G. & Chavakis, T. Endogenous modulators of inflammatory cell recruitment. *Trends Immunol.* **34**, 1–6 (2013).
- Shin, J. et al. DEL-1 restrains osteoclastogenesis and inhibits inflammatory bone loss in nonhuman primates. *Sci Transl. Med.* **7**, 307ra155 (2015).
- Mitroulis, I. et al. Secreted protein Del-1 regulates myelopoiesis in the hematopoietic stem cell niche. *J. Clin. Invest.* **127**, 3624–3639 (2017).
- Choi, E. Y. et al. Del-1, an endogenous leukocyte-endothelial adhesion inhibitor, limits inflammatory cell recruitment. *Science* **322**, 1101–1104 (2008).
- Mitroulis, I. et al. Developmental endothelial locus-1 attenuates complement-dependent phagocytosis through inhibition of Mac-1-integrin. *Thromb. Haemost.* **111**, 1004–1006 (2014).
- Choi, E. Y. et al. Developmental endothelial locus-1 is a homeostatic factor in the central nervous system limiting neuroinflammation and demyelination. *Mol. Psychiatry* **20**, 880–888 (2014).
- Eskan, M. A. et al. The leukocyte integrin antagonist Del-1 inhibits IL-17-mediated inflammatory bone loss. *Nat. Immunol.* **13**, 465–473 (2012).
- Kang, Y.-Y., Kim, D.-Y., Lee, S.-H. & Choi, E. Y. Deficiency of developmental endothelial locus-1 (Del-1) aggravates bleomycin-induced pulmonary fibrosis in mice. *Biochem. Biophys. Res. Commun.* **445**, 369–374 (2014).
- Kourtzelis, I. et al. Developmental endothelial locus-1 modulates platelet-monocyte interactions and instant blood-mediated inflammatory reaction in islet transplantation. *Thromb. Haemost.* **115**, 781–788 (2016).
- Maekawa, T. et al. Antagonistic effects of IL-17 and D-resolvins on endothelial Del-1 expression through a GSK-3 β -C/EBP β pathway. *Nat. Commun.* **6**, 8272 (2015).
- Folwaczny, M., Karnesi, E., Berger, T. & Paschos, E. Clinical association between chronic periodontitis and the leukocyte extravasation inhibitors developmental endothelial locus-1 and pentraxin-3. *Eur. J. Oral Sci.* **125**, 258–264 (2017).
- Hajishengallis, G., Moutsopoulos, N. M., Hajishengallis, E. & Chavakis, T. Immune and regulatory functions of neutrophils in inflammatory bone loss. *Semin. Immunol.* **28**, 146–158 (2016).
- Kantarci, A. & Van Dyke, T. E. Resolution of inflammation in periodontitis. *J. Periodontol.* **76**, 2168–2174 (2005).
- Kajikawa, T. et al. Milk fat globule epidermal growth factor 8 inhibits periodontitis in non-human primates and its gingival crevicular fluid levels can differentiate periodontal health from disease in humans. *J. Clin. Periodontol.* **44**, 472–483 (2017).
- Cohen, R. E., Research, Science and Therapy Committee, American Academy of Periodontology. Position paper: periodontal maintenance. *J. Periodontol.* **74**, 1395–1401 (2003).
- Hajishengallis, G., Lamont, R. J. & Graves, D. T. The enduring importance of animal models in understanding periodontal disease. *Virulence* **6**, 229–235 (2015).
- Ariel, A. & Timor, O. Hanging in the balance: endogenous anti-inflammatory mechanisms in tissue repair and fibrosis. *J. Pathol.* **229**, 250–263 (2013).
- Choi, E. Y. et al. Regulation of LFA-1-dependent inflammatory cell recruitment by Cbl-b and 14-3-3 proteins. *Blood* **111**, 3607–3614 (2008).
- Getting, S. J. et al. Molecular determinants of monosodium urate crystal-induced murine peritonitis: a role for endogenous mast cells and a distinct requirement for endothelial-derived selectins. *J. Pharmacol. Exp. Ther.* **283**, 123–130 (1997).
- Martin, W. J., Shaw, O., Liu, X., Steiger, S. & Harper, J. L. Monosodium urate monohydrate crystal-recruited noninflammatory monocytes differentiate into M1-like proinflammatory macrophages in a peritoneal murine model of gout. *Arthritis Rheum.* **63**, 1322–1332 (2011).
- Serhan, C. N., Chiang, N. & Van Dyke, T. E. Resolving inflammation: dual anti-inflammatory and pro-resolution lipid mediators. *Nat. Rev. Immunol.* **8**, 349–361 (2008).
- Dalli, J. et al. Resolvin D3 and aspirin-triggered resolvin D3 are potent immunoresolvents. *Chem. Biol.* **20**, 188–201 (2013).
- Bannenberg, G. L. et al. Molecular circuits of resolution: formation and actions of resolvins and protectins. *J. Immunol.* **174**, 4345–4355 (2005).
- Hong, S. et al. Resolvin E1 metabolome in local inactivation during inflammation-resolution. *J. Immunol.* **180**, 3512–3519 (2008).
- Villoutreix, B. O. & Miteva, M. A. Discoidin domains as emerging therapeutic targets. *Trends Pharmacol. Sci.* **37**, 641–659 (2016).
- Lastrucci, C. et al. Molecular and cellular profiles of the resolution phase in a damage-associated molecular pattern (DAMP)-mediated peritonitis model and revelation of leukocyte persistence in peritoneal tissues. *FASEB J.* **29**, 1914–1929 (2015).
- Savill, J., Dransfield, I., Hogg, N. & Haslett, C. Vitronectin receptor-mediated phagocytosis of cells undergoing apoptosis. *Nature* **343**, 170–173 (1990).
- Mevorach, D., Mascarenhas, J. O., Gershov, D. & Elkon, K. B. Complement-dependent clearance of apoptotic cells by human macrophages. *J. Exp. Med.* **188**, 2313–2320 (1998).
- Stables, M. J. et al. Transcriptomic analyses of murine resolution-phase macrophages. *Blood* **118**, e192–e208 (2011).
- Rébé, C. et al. Induction of transglutaminase 2 by a liver X receptor/retinoic acid receptor α pathway increases the clearance of apoptotic cells by human macrophages. *Circ. Res.* **105**, 393–401 (2009).
- Hanayama, R., Tanaka, M., Miwa, K. & Nagata, S. Expression of developmental endothelial locus-1 in a subset of macrophages for engulfment of apoptotic cells. *J. Immunol.* **172**, 3876–3882 (2004).
- Rosas, M. et al. The transcription factor Gata6 links tissue macrophage phenotype and proliferative renewal. *Science* **344**, 645–648 (2014).
- Hajishengallis, G. Periodontitis: from microbial immune subversion to systemic inflammation. *Nat. Rev. Immunol.* **15**, 30–44 (2015).
- Chiang, N. et al. Infection regulates pro-resolving mediators that lower antibiotic requirements. *Nature* **484**, 524–528 (2012).
- Hasturk, H. et al. Resolvin E1 regulates inflammation at the cellular and tissue level and restores tissue homeostasis in vivo. *J. Immunol.* **179**, 7021–7029 (2007).
- A-Gonzalez, N. et al. Apoptotic cells promote their own clearance and immune tolerance through activation of the nuclear receptor LXR. *Immunity* **31**, 245–258 (2009).
- Kidani, Y. & Bensinger, S. J. Liver X receptor and peroxisome proliferator-activated receptor as integrators of lipid homeostasis and immunity. *Immunol. Rev.* **249**, 72–83 (2012).
- Choi, J.-Y. et al. Mer signaling increases the abundance of the transcription factor LXR to promote the resolution of acute sterile inflammation. *Sci. Signal.* **8**, ra21 (2015).
- Hong, C. et al. Constitutive activation of LXR in macrophages regulates metabolic and inflammatory gene expression: identification of ARL7 as a direct target. *J. Lipid Res.* **52**, 531–539 (2011).
- Hidai, C., Kawana, M., Kitano, H. & Kokubun, S. Discoidin domain of Del1 protein contributes to its deposition in the extracellular matrix. *Cell Tissue Res.* **330**, 83–95 (2007).
- Galli, S. J., Borregaard, N. & Wynn, T. A. Phenotypic and functional plasticity of cells of innate immunity: macrophages, mast cells and neutrophils. *Nat. Immunol.* **12**, 1035–1044 (2011).
- Matzinger, P. & Kamala, T. Tissue-based class control: the other side of tolerance. *Nat. Rev. Immunol.* **11**, 221–230 (2011).

Acknowledgements

This work was supported by grants from the European Research Council (DEMETINL to T.C.), the Deutsche Forschungsgemeinschaft (Transregio-SFB 83 to Ü.C. as well as Transregio-SFB 127 and Transregio-SFB 205 to T.C.), and the National Institutes of Health (AI068730, DE024153, DE024716, DE026152, and DE015254 to G.H.). I.K. was supported by the MeDDriveGrant (60.400) from the Technische Universität Dresden Medical Faculty. A.Castrillo was supported by Spanish MINECO SAF2014-56819R and SAF2015-71878-REDT. This work was supported in part by intramural National Institute of Dental and Craniofacial Research, National Institutes of Health funding. We thank R. Naumann (Transgenic Core Facility, Max-Planck Institute for Cell Biology and Genetics Dresden, Germany) for microinjections and B. Gercken and M. Schuster (Institute for Clinical Chemistry and Laboratory Medicine, Faculty of Medicine, Technische Universität Dresden, Dresden, Germany) for technical assistance. Parts of this work are included in the master's theses of C.D. at the Technische Universität Dresden, Dresden, Germany, and A.F. at the University of Porto, Porto, Portugal.

Author contributions

I.K. designed the study, performed experiments, analyzed and interpreted data, and wrote the manuscript; X.L. and I.M. designed and performed experiments and analyzed and interpreted data; D.G. generated reagents and performed experiments; T.K. performed experiments and analyzed and interpreted data; B.Wang and J.M.K. designed experiments and interpreted data; M.G., J.v.R., A.Czogalla, A.F., and C.D. performed experiments and interpreted data; M.T., K.R., L.-S.C., and K.-J.C. performed experiments; K.H. and S.G. generated critical reagents and performed experiments; J.-H.L. and A.K.T. interpreted data; L.A.B.J., N.M.M., B.Wielockx, and A.Castrillo contributed to experimental design and interpreted data; Ü.C. supervised research, designed experiments, and interpreted data; and G.H. and T.C. conceived and designed the study, supervised research, interpreted data, and wrote the paper.

Competing interests

The authors declare no competing interests.

Additional information

Supplementary information is available for this paper at <https://doi.org/10.1038/s41590-018-0249-1>.

Reprints and permissions information is available at www.nature.com/reprints.

Correspondence and requests for materials should be addressed to I.K. or G.H. or T.C.

Publisher's note: Springer Nature remains neutral with regard to jurisdictional claims in published maps and institutional affiliations.

© The Author(s), under exclusive licence to Springer Nature America, Inc. 2018

Methods

Human subjects and GCF sample collection. Research procedures were performed in compliance with all relevant ethical regulations under a protocol approved by the institutional review board of the University of Pennsylvania. Signed informed consent was obtained to procure GCF from individuals treated in the postgraduate clinic of the Department of Periodontics, University of Pennsylvania School of Dental Medicine. All subjects were at least 28 years old with no serious medical illness contraindicative of periodontal treatment. The inclusion criteria for chronic periodontitis were diseased sites with probing pocket depth ≥ 5 mm associated with clinical attachment loss ≥ 4 mm, presence of bleeding on probing, and radiographic evidence of bone loss. GCF was collected from 7 patients (3 male and 4 female) prior to initiation of SRP and at a re-evaluation appointment 6 weeks later. To collect GCF, teeth were dried and isolated with cotton rolls and samples were collected from distinct periodontitis-involved sites using PerioPaper strips (OraFlow). The strips were placed in the selected sites until mild resistance was felt and were kept in place for 30 s, as previously described^{40,51}. Samples contaminated with blood or saliva were discarded. Each PerioPaper strip was placed into a coded sealed polypropylene tube containing 0.1 ml PBS with proteinase inhibitors. The samples were placed at 4°C for 2 h and then stored at -80°C until analysis.

Mice. Mice were housed under specific pathogen-free conditions on a standard 12/12 h light/dark cycle. Sex-matched mice that were 8–10 weeks old were used. Food and water were provided ad libitum. In experiments where only wild-type C57BL/6 mice were used, these were purchased from Janvier Labs or the Jackson Laboratory. *Del1*^{KO} mice and mice overexpressing DEL-1 in the endothelium (EC-Del1; generated by using a Tie2 promoter/enhancer construct) have been previously described^{11,16,52,53}. Mice overexpressing in macrophages full-length DEL-1 (CD68-Del1) or the truncated version of DEL-1 that lacks the discoidin I-like domains (CD68-Del1-[E1-E3]) were generated in a C57BL/6N background, using the human CD68 promoter^{54,55}. The CD68-IVS1 promoter construct was subcloned into the pUC19 vector backbone. Mouse *Edil3* (encoding full-length DEL-1 and E1-E3 derivative) were amplified by PCR, and *Edil3* complementary DNA (full length or E1-E3) was cloned into the pUC19-CD68 vector and subsequently amplified in *Escherichia coli* strain DH5 α . For generation of transgenic mice, the constructs were linearized and microinjected into pronuclei of mouse oocytes (C57BL/6N.Crl). Offspring were genotyped by PCR, and transgene-bearing founders were further crossed with C57BL/6N mice (Charles River Laboratories). Following screening for transgene transmission to the offspring and *Del1* overexpression by quantitative PCR, two founders from each strain (CD68-Del1 and CD68-Del1-[E1-E3]) were selected. Data are presented from one founder per strain; key experiments were repeated using the second founder in each case, and similar results were obtained. Mice deficient in α_1 integrin (*Itga1*^{KO}) or α_M integrin (*Itgam*^{KO}) were previously described^{11,12,56,57}. Mice deficient in β_3 integrin (*Itgb3*^{KO}) and their respective wild-type control mice were obtained from the Jackson Laboratory. Mice deficient in both LXR isoforms (*Nr1h3*^{KO}*Nr1h2*^{KO}; here referred to as *Lxra-Lxrb*^{DKO}) in a C57BL/6 background^{45,58} were originally provided from D. Mangelsdorf (University of Texas Southwestern). All animal experiments were performed in compliance with all relevant ethical regulations. Specifically, *Lxra-Lxrb*^{DKO} mice and their respective wild-type control mice were housed and used in accordance with the CSIC and ULPGC animal research committees; all other animal procedures were approved by the Landesdirektion Sachsen, Germany, or the Institutional Animal Care and Use Committee of the University of Pennsylvania.

MSU crystals. MSU crystals were prepared as described³⁹. Briefly, uric acid (Sigma-Aldrich) was added to H₂O containing NaOH, and the solution was boiled until dissolution was reached. Afterwards, the solution was passed through a 0.2 μ m filter and NaCl was added. After 7 d of storage at 26°C, crystals were washed with ethanol and their shape was examined using microscopy.

MSU peritonitis and treatment of mice with antibodies and proteins. MSU crystals (3 mg) were injected intraperitoneally in mice, and peritoneal exudates were collected at different time points (8, 24, 36 h) for the analysis of inflammatory cell composition. To examine the role of $\alpha_M\beta_2$ integrin in MSU crystal-induced leukocyte recruitment, 50 μ g of a blocking antibody to α_M integrin (clone M1/70; BioLegend) or an isotype control (clone RTK4530; BioLegend) were injected intravenously in mice 10 min prior to intraperitoneal administration of the MSU crystals. Mice were killed, and peritoneal exudates were analyzed 8 h after the MSU crystal injection.

The effect of DEL-1 on the regulation of resolution of MSU crystal-induced inflammation was investigated by injecting 5 μ g of either DEL-1-Fc or Fc control intraperitoneally 20 h after the treatment of mice with MSU crystals. Mice were killed 4 h after DEL-1-Fc injection, and clearance of apoptotic neutrophils was evaluated in peritoneal exudates.

In other experiments, 300 ng of RvD1 or vehicle control (PBS) was administered intraperitoneally together with MSU crystals in wild-type and *Del1*^{KO} mice. 24 h after injection, the numbers of apoptotic neutrophils were measured in peritoneal exudates.

Resolving and non-resolving model of LIP in mice. The placement of ligatures accelerates bacteria-mediated inflammation and bone loss⁶⁰. To induce ligature-induced periodontitis, a 5-0 silk ligature was tied around the maxillary left second molar of mice, as previously described⁶¹. The contralateral molar tooth in each mouse was left unligated to serve as baseline control for bone loss measurements and gingival gene expression. The ligatures remained in place for 5 or 10 d (5DL and 10DL groups, respectively). In another group, ligatures were removed at day 5 to allow transition to inflammation resolution, and the mice were monitored for another 5 d (5DL-5DR group). The animals were euthanized at various time points up to day 10 as specified in figure legends. Defleshed maxillae were used to measure bone heights (that is, the distances from the cemento-enamel junction (CEJ) to the alveolar bone crest (ABC)) at six predetermined points on the ligated site as previously described⁶¹. To calculate bone loss, the six-site total CEJ-ABC distance for the ligated site of each mouse was subtracted from the six-site total CEJ-ABC distance of the contralateral unligated site. The results were presented in millimeters, and negative values indicate bone loss relative to the baseline (unligated control). Excised gingival tissue was used to extract total RNA using the RNeasy Mini Kit (Qiagen). The RNA was quantified by spectrometry at 260 and 280 nm and was reverse-transcribed using the High Capacity RNA-to-cDNA Kit (Life Technologies). Quantitative real-time PCR with cDNA was performed using the Applied Biosystems 7500 Fast Real-Time PCR System according to the manufacturer's protocol (Life Technologies). Data were analyzed using the comparative ($\Delta\Delta C_t$) method. TaqMan probes, sense primers, and antisense primers for detection and quantification of genes investigated in Fig. 2a and Supplementary Fig. 1c were purchased from Life Technologies. Mouse GCF was collected according to a previously described method⁶². Briefly, a fresh ligature was placed in the gingival crevice for 10 min, and the collected GCF was eluted in a solution of PBS containing 1% Triton-X-100. Coronal sections of maxillae and intact surrounding gingival tissue from wild-type and *Del1*^{KO} mice were prepared as previously described⁶³ and stained with a primary monoclonal antibody to Ly6G (clone RB6-8C5; eBioscience) followed by a secondary goat anti-rat immunoglobulin G (IgG) antibody conjugated to Alexa Fluor 488. Ly6G⁺ cells were enumerated from three random sections from each of six mice per time point per genotype.

Isolation and culture of primary human and mouse cells. *Human monocyte-derived macrophages.* To prepare human monocyte-derived macrophages (MDMs), peripheral blood mononuclear cells were isolated from healthy donors by density gradient separation using Histopaque 1077 (Sigma-Aldrich). To induce differentiation to macrophages, cells were plated and cultured in the presence of 20 ng ml⁻¹ human macrophage colony stimulating factor (eBioscience) for 4 d.

Human neutrophils. Neutrophils were isolated from peripheral blood of healthy donors using double gradient separation (Histopaque 1119 and 1077; Sigma-Aldrich). To induce apoptosis, purified cells were incubated in complete culture medium overnight at 37°C. Apoptotic rate was confirmed with annexin V staining (eBioscience).

Peripheral blood was collected from healthy volunteers in compliance with relevant ethical regulations (after written informed consent; the procedure was approved by the ethics committee of the Technische Universität Dresden).

Mouse BMDMs and neutrophils. Bone marrow cells were flushed from femurs and tibiae of wild-type, CD68-Del1, CD68-Del1-[E1-E3], or different knockout mice. After lysis of erythrocytes using red blood cell lysis buffer (eBioscience), cells were plated and cultured in the presence of recombinant mouse granulocyte macrophage colony-stimulating factor (20 ng ml⁻¹; eBioscience). Culture medium was replaced every 2 d, and after 7 d differentiated BMDMs were used for further experiments^{25,56}. To isolate neutrophils, bone marrow cells, after erythrocyte lysis, were centrifuged in 62% Percoll gradient (GE Healthcare). Induction of apoptosis was performed after overnight culture of the obtained neutrophil population in HBSS containing 1% FBS.

Isolated peritoneal macrophages. For peritoneal macrophage isolation, peritoneal fluid was obtained from untreated *Del1*^{KO}, CD68-Del1, or CD68-Del1-[E1-E3] mice and their respective wild-type controls. Isolated peritoneal cells were plated and cultured overnight. Culture medium was then removed, cells were washed in PBS, and the adherent cell population was used in *in vitro* efferocytosis assays and gene expression analyses.

Efferocytosis assays. *In vitro.* *In vitro* analysis of efferocytosis as well as subsequent gene and protein expression analysis in efferocytic macrophages was performed as previously described^{43,64-66}. Human MDMs or mouse wild-type BMDMs were pretreated with DEL-1-Fc, DEL-1[E1-E3]-Fc, DEL-1[RGE]-Fc, or Fc control protein for 15 min in 96-well plates. Apoptotic neutrophils were stained with 1 μ g ml⁻¹ BCECF acetoxymethyl ester (Thermo Fisher Scientific). Afterwards, human MDMs or mouse wild-type BMDMs were co-cultured with apoptotic neutrophils of human or mouse origin, respectively, in a 5:1 ratio of apoptotic neutrophils to macrophages (unless otherwise indicated) for 30 min. In other experiments, isolated peritoneal macrophages (see 'Isolation and culture of primary human and

mouse cells⁷) from *Del1*^{KO} or CD68-Del1 mice, or from the corresponding wild-type controls, were incubated with apoptotic neutrophils as described above for BMDMs. Macrophages were then washed three times with PBS and fixed with 4% paraformaldehyde for 30 min. Efferocytosis index was evaluated using microscopy (Axio Observer Z1 microscope, Carl Zeiss). Zeiss ZEN 2012 (blue edition) software was used for collection and analysis of images. In some cases, ImageJ software was also used for image analysis. At least three different fields per sample were analyzed, and at least 30 macrophages per field were evaluated.

For gene expression analysis, macrophages were incubated with apoptotic neutrophils for 3 h; thereafter, macrophages were washed three times with PBS prior to RNA isolation. For protein analysis, macrophages were incubated with apoptotic neutrophils for 3 h in serum-free medium; thereafter, the cell-free supernatant of the co-culture was collected and analyzed by ELISA.

Intervention studies were performed by treating BMDMs with a selective antagonist for LXR (1 μ M; Axon) for 15 min prior to the addition of DEL-1 proteins.

In order to examine the effect of LFA-1, Mac-1, or ICAM-1 on DEL-1-dependent efferocytosis, isolated peritoneal macrophages from CD68-Del1 and litter-mate wild-type mice were incubated with apoptotic neutrophils in the presence of isotype controls or a neutralizing antibody (10 μ g ml⁻¹ each) to LFA-1 integrin (clone 17/4), Mac-1 integrin (clone M1/70), or ICAM-1 (clone YN1/1.7.4). Apoptotic neutrophils were added to the macrophage culture for 30 min. Macrophages were then washed, and efferocytosis index was evaluated, as described above.

In vivo. Wild-type mice were injected intraperitoneally with 2% w/v thioglycolate (Sigma-Aldrich). After 72 h, animals received intraperitoneally 5×10^6 apoptotic neutrophils that were pre-stained with BCECF acetoxymethyl ester, together with 5 μ g of either Fc control or DEL-1-Fc; 3 h after the latter injection, mice were killed, and the efferocytosis index was analyzed in the peritoneal exudates with flow cytometry. Phagocytic macrophages were identified as BCECF⁺F4/80⁺ cells.

DEL-1 proteins. Full-length human DEL-1 was generated and purified as a fusion protein with the human IgG1-Fc fragment (DEL-1-Fc) as described^{9,10}. DEL-1 that lacks the discoidin 1-like domains (DEL-1[E1-E3]-Fc) and a point mutant protein in which Glu was substituted for Asp in the RGD motif of the second EGF-like repeat (DEL-1[RGE]-Fc) were prepared as previously described⁹. Recombinant human DEL-1 and IgG Fc protein were purchased from R&D Systems.

Liposome preparation and quality control. Chloroform (Roth)/methanol (VWR) (10/1) solutions of 1-palmitoyl-2-oleoyl-sn-glycero-3-phosphocholine (POPC; Avanti Polar Lipids), 1-palmitoyl-2-oleoyl-sn-glycero-3-phospho-L-serine (POPS; Avanti Polar Lipids) and cholesterol (Chol; Sigma-Aldrich), were mixed in a molar ratio of 60:40 (POPC:Chol) or 55:40:5 (POPC:Chol:POPS) with a total lipid content of 1 mg. The solvent was evaporated under a gentle nitrogen stream to form a uniform lipid film and further dried under vacuum for at least 1 h. The lipid film was rehydrated in 1 ml of HBS (25 mM HEPES, 150 mM NaCl, pH 7.4), subjected to 11 freeze-thaw cycles and extruded 21 times through a 100 nm membrane (Whatman).

The quality of liposomes was checked by thin-layer chromatography (Supplementary Fig. 6c); therefore, 30 μ l of liposomes were extracted with 90 μ l chloroform:methanol (1:1). The lower organic phase was collected and loaded on a silica plate (Merck). Lipids were separated in a solvent mixture of chloroform:ethanol:water:triethylamine (30:35:7:35 v/v). The dried plate was stained with primuline (Sigma-Aldrich; 5 mg in 100 ml acetone:water (80:20)), and the fluorescence was recorded on a Typhoon 9410 (Amersham Bioscience).

For ζ -potential measurements (Supplementary Fig. 6d), liposomes were diluted 10 times in water (ZetaSizer; Malvern Panalytical).

In vitro lipid binding assay. The binding assay was performed using a platform from Meso Scale Discovery. Liposomes were passively adsorbed on the electrode surface for 1 h at 23 °C, and the residual sites on the surface were blocked for 1 h with 0.2% (w/v) porcine gelatin (Sigma-Aldrich) in HBS. After three wash steps with HBS, a serial dilution of recombinant DEL-1 in blocking buffer, covering the desired range, was applied and incubated for 2 h. Unbound protein was removed, and rabbit anti-DEL-1 serum (1:2,000 in blocking buffer) was applied for 1 h followed by three wash steps with HBS. For detection, a goat anti-rabbit secondary antibody conjugated with Sulfo-Tag (Meso Scale Discovery) was used at 1.25 μ g ml⁻¹ in blocking buffer for 1 h in the dark. Free secondary antibody was washed off, and reading buffer (surfactant-free reading buffer from Meso Scale Discovery) was added. The readout was performed on a SECTOR Imager 6000 chemiluminescence reader. The resulting data were analyzed with GraphPad Prism6. A non-linear curve fitting was applied, and the binding kinetics were calculated using one-sited total and non-specific binding; the binding of DEL-1 to PC vesicles was defined as background.

Flow cytometry and sorting. Antibodies to CD11b (clone M1/70; BD Biosciences), Ly-6G (clone 1A8; BD Biosciences), CD115 (clone AFS98; BioLegend), ICAM-2 (CD102; clone 3C4 (mIC2/4); BD Biosciences), and F4/80 (clone BM8; eBioscience) were used for flow cytometry⁶⁷. Antibody to mouse

CD16/32 was used to block Fc γ receptors (clone 2.4G2; BD Biosciences). Peritoneal neutrophils were identified as Ly-6G⁺CD11b⁺ cells. Peritoneal monocytes/macrophages from MSU crystal-treated mice were defined as Ly-6G⁺CD11b⁺ cells after excluding the SSC^{hi} eosinophil population⁶⁸ (gate R3 in Supplementary Fig. 2a; cells in R3 were identified as eosinophils by additional Siglec-F staining (not shown)). Apoptotic neutrophils were detected using an annexin V apoptosis detection kit (eBioscience), and cell viability was determined after staining with Hoechst 33258 (Thermo Fisher Scientific). Flow cytometric analysis of stained cells was performed on a FACS Canto II flow cytometer (BD Biosciences). After the removal of erythrocytes with red blood cell lysis buffer (eBioscience), cells from the peritoneal exudates were pre-incubated with anti-mouse CD16/CD32 and then incubated with antibodies to specific surface receptors in PBS supplemented with 5% FBS (Life Technologies).

Cell sorting was performed using a FACS Aria cell sorter (BD Biosciences) to >95% purity. Peritoneal monocytes/macrophages from MSU crystal-treated mice, defined as above, were sorted at 24 h after the induction of MSU crystal-induced inflammation. In other experiments, macrophages were sorted as CD11b⁺F4/80⁺ cells from peritoneal fluids of untreated mice (not subjected to MSU crystal-induced inflammation). GATA-6⁺ resident macrophages in peritoneal fluids of untreated mice were characterized and sorted as the CD115⁺ICAM-2⁻ cells, as previously described⁶⁹. In addition, CD115⁺ICAM-2⁻ macrophages were sorted from peritoneum of untreated mice. Data analysis was performed using FlowJo software (Tree Star).

Quantitative real-time PCR. Total RNA was extracted from cultured or sorted cells and was quantified by spectrometry at 260 and 280 nm. cDNA was synthesized using the iScript cDNA Synthesis Kit (Bio-Rad) or the High Capacity RNA-to-cDNA Kit (Life Technologies). Real-time PCR was performed using the SsoFast EvaGreen Supermix (BioRad) and gene-specific primers (Supplementary Table 1) in a CFX384 real-time PCR detection system (BioRad). The internal control for normalization was 18S ribosomal RNA⁵⁶. Data were analyzed using the $\Delta\Delta$ Ct method.

ELISAs. Mouse IL-6, IL-17A, TGF- β 1, and TGF- β 2 proteins were measured in gingival tissue lysates using kits from eBioscience or R&D Systems. TGF- β 1 protein in cell culture supernatants was assessed with ELISA using a commercially available kit (BioLegend). The DEL-1 concentrations in mouse GCF, supernatants of peritoneal exudates, and isolated peritoneal macrophage cultures were determined using a sandwich ELISA, as previously described⁷. Specificity of this ELISA was confirmed as shown in Supplementary Fig. 1b. Concentrations of SPMs were measured in mouse GCF and supernatant of peritoneal exudates using commercially available ELISA kits (Cayman Chemical for RvD1, MyBioSource for RvE1, and Neogen for lipoxin A4). According to the manufacturers, the ELISA for lipoxin A4 exhibits 24% cross-reactivity for 15-*epi*-lipoxin A4, 5% for 5S,6R-DiHETE, and 1% for lipoxin B4; the ELISA for RvD1 has 20% cross-reactivity for 5S,6R-lipoxin A4, 4.2% for (17R)-resolvin D1, and 0.7% for 10S,17S-DiHDoHE. Minor cross-reactivities ($\leq 0.1\%$) of both lipoxin A4 and RvD1 also exist for other SPMs or analogs thereof. According to the manufacturer, no significant cross-reactivity between RvE1 and analogs has been observed, although cross-reactivities cannot be formally excluded. At the time of analysis for human DEL-1 content of collected GCF from periodontitis patients, 1% Triton X-100 was added to the buffer in each tube sample and incubated at 4 °C for 2 h to elute the GCF contents. After centrifugation (500 g for 5 min), the concentration of human DEL-1 in the eluted GCF samples was measured using an ELISA kit according to the instructions of the manufacturer (R&D Systems).

Statistics. Results are presented as mean \pm s.e.m. Data were analyzed by two-tailed Student's *t*-test or two-tailed Mann-Whitney *U*-test, as appropriate (after testing for normality). Multiple-group comparisons were performed using analysis of variance (ANOVA) and the Dunnett's, Tukey's, or Sidak's multiple comparison tests. Analysis of human GCF samples (Fig. 1) and probing pocket depth (Supplementary Fig. 1a) was performed by pre-post paired two-way ANOVA with repeated measures by patient. All statistical analyses were performed on GraphPad Prism software. *P* values <0.05 were considered to be statistically significant.

Reporting Summary. Further information on research design is available in the Nature Research Reporting Summary linked to this article.

Data availability:

The data that support the findings of this study are available from the corresponding authors upon reasonable request.

References

- Griffiths, G. S. Formation, collection and significance of gingival crevice fluid. *Periodontol.* 2000 31, 32–42 (2003).
- Bostanci, N. et al. Gingival crevicular fluid levels of RANKL and OPG in periodontal diseases: implications of their relative ratio. *J. Clin. Periodontol.* 34, 370–376 (2007).

52. Subramanian, P. et al. Endothelial cell-specific overexpression of developmental endothelial locus-1 does not influence atherosclerosis development in ApoE^{-/-} mice. *Thromb. Haemost.* **117**, 2003–2005 (2017).
53. Chen, L. S. et al. Endothelial cell-specific overexpression of Del-1 drives expansion of haematopoietic progenitor cells in the bone marrow. *Thromb. Haemost.* **118**, 613–616 (2018).
54. Lang, R., Rutschman, R. L., Greaves, D. R. & Murray, P. J. Autocrine deactivation of macrophages in transgenic mice constitutively overexpressing IL-10 under control of the human CD68 promoter. *J. Immunol.* **168**, 3402–3411 (2002).
55. Gough, P. J., Gordon, S. & Greaves, D. R. The use of human CD68 transcriptional regulatory sequences to direct high-level expression of class A scavenger receptor in macrophages in vitro and in vivo. *Immunology* **103**, 351–361 (2001).
56. Chung, K.-J. et al. A self-sustained loop of inflammation-driven inhibition of beige adipogenesis in obesity. *Nat. Immunol.* **18**, 654–664 (2017).
57. Coxon, A. et al. A novel role for the $\beta 2$ integrin CD11b/CD18 in neutrophil apoptosis: a homeostatic mechanism in inflammation. *Immunity* **5**, 653–666 (1996).
58. A-Gonzalez, N. et al. The nuclear receptor LXR α controls the functional specialization of splenic macrophages. *Nat. Immunol.* **14**, 831–839 (2013).
59. Joosten, L. A. B. et al. Engagement of fatty acids with Toll-like receptor 2 drives interleukin-1 β production via the ASC/caspase 1 pathway in monosodium urate monohydrate crystal-induced gouty arthritis. *Arthritis Rheum.* **62**, 3237–3248 (2010).
60. Graves, D. T., Fine, D., Teng, Y.-T. A., Van Dyke, T. E. & Hajishengallis, G. The use of rodent models to investigate host-bacteria interactions related to periodontal diseases. *J. Clin. Periodontol.* **35**, 89–105 (2008).
61. Abe, T. & Hajishengallis, G. Optimization of the ligature-induced periodontitis model in mice. *J. Immunol. Methods* **394**, 49–54 (2013).
62. Matsuda, S. et al. A novel method of sampling gingival crevicular fluid from a mouse model of periodontitis. *J. Immunol. Methods* **438**, 21–25 (2016).
63. Abe, T. et al. The B cell-stimulatory cytokines BlyS and APRIL are elevated in human periodontitis and are required for B cell-dependent bone loss in experimental murine periodontitis. *J. Immunol.* **195**, 1427–1435 (2015).
64. Mukundan, L. et al. PPAR- δ senses and orchestrates clearance of apoptotic cells to promote tolerance. *Nat. Med.* **15**, 1266–1272 (2009).
65. Xiong, W., Frasch, S. C., Thomas, S. M., Bratton, D. L. & Henson, P. M. Induction of TGF- $\beta 1$ synthesis by macrophages in response to apoptotic cells requires activation of the scavenger receptor CD36. *PLoS ONE* **8**, e72772 (2013).
66. Fadok, V. A. et al. Macrophages that have ingested apoptotic cells in vitro inhibit proinflammatory cytokine production through autocrine/paracrine mechanisms involving TGF- β , PGE2, and PAF. *J. Clin. Investig.* **101**, 890–898 (1998).
67. Mitroulis, I. et al. Modulation of myelopoiesis progenitors is an integral component of trained immunity. *Cell* **172**, 147–161 (2018).
68. Davies, L. C. et al. A quantifiable proliferative burst of tissue macrophages restores homeostatic macrophage populations after acute inflammation. *Eur. J. Immunol.* **41**, 2155–2164 (2011).
69. Gautier, E. L. et al. Gata6 regulates aspartoacylase expression in resident peritoneal macrophages and controls their survival. *J. Exp. Med.* **211**, 1525–1531 (2014).

Reporting Summary

Nature Research wishes to improve the reproducibility of the work that we publish. This form provides structure for consistency and transparency in reporting. For further information on Nature Research policies, see [Authors & Referees](#) and the [Editorial Policy Checklist](#).

Statistical parameters

When statistical analyses are reported, confirm that the following items are present in the relevant location (e.g. figure legend, table legend, main text, or Methods section).

n/a Confirmed

- The exact sample size (n) for each experimental group/condition, given as a discrete number and unit of measurement
- An indication of whether measurements were taken from distinct samples or whether the same sample was measured repeatedly
- The statistical test(s) used AND whether they are one- or two-sided
Only common tests should be described solely by name; describe more complex techniques in the Methods section.
- A description of all covariates tested
- A description of any assumptions or corrections, such as tests of normality and adjustment for multiple comparisons
- A full description of the statistics including central tendency (e.g. means) or other basic estimates (e.g. regression coefficient) AND variation (e.g. standard deviation) or associated estimates of uncertainty (e.g. confidence intervals)
- For null hypothesis testing, the test statistic (e.g. F , t , r) with confidence intervals, effect sizes, degrees of freedom and P value noted
Give P values as exact values whenever suitable.
- For Bayesian analysis, information on the choice of priors and Markov chain Monte Carlo settings
- For hierarchical and complex designs, identification of the appropriate level for tests and full reporting of outcomes
- Estimates of effect sizes (e.g. Cohen's d , Pearson's r), indicating how they were calculated
- Clearly defined error bars
State explicitly what error bars represent (e.g. SD, SE, CI)

Our web collection on [statistics for biologists](#) may be useful.

Software and code

Policy information about [availability of computer code](#)

Data collection	BD FACS Diva v6.1.3 software and Zeiss ZEN 2012 (blue edition) were used for cytofluorimetric data and image collection, respectively.
Data analysis	FlowJo version 9.3.2 GraphPad prism version 5 and version 7 Image J version 1.46r

For manuscripts utilizing custom algorithms or software that are central to the research but not yet described in published literature, software must be made available to editors/reviewers upon request. We strongly encourage code deposition in a community repository (e.g. GitHub). See the Nature Research [guidelines for submitting code & software](#) for further information.

Data

Policy information about [availability of data](#)

All manuscripts must include a [data availability statement](#). This statement should provide the following information, where applicable:

- Accession codes, unique identifiers, or web links for publicly available datasets
- A list of figures that have associated raw data
- A description of any restrictions on data availability

The data that support the findings of this study are available from the corresponding authors upon request.

Field-specific reporting

Please select the best fit for your research. If you are not sure, read the appropriate sections before making your selection.

Life sciences Behavioural & social sciences Ecological, evolutionary & environmental sciences

For a reference copy of the document with all sections, see [nature.com/authors/policies/ReportingSummary-flat.pdf](https://www.nature.com/authors/policies/ReportingSummary-flat.pdf)

Life sciences study design

All studies must disclose on these points even when the disclosure is negative.

Sample size	No statistical methods were used to predetermine sample size. An estimate of three to seven (or more) mice per group were used in individual experiments and assumed this sample size would be required to recognize differences between genotypes and treatments.
Data exclusions	No data excluded.
Replication	Experiments were reliably reproduced; in particular, most of the experiments were repeated yielding similar results.
Randomization	For experiments comparing transgenic or knockout mice vs. wild-type controls, the groups were set up based on genotype. In the experiments where mice were treated with Fc or Del-1-Fc or in the experiments where mice were treated with RvD1 or PBS, groups were randomly assigned to the two different treatments.
Blinding	The investigators were not blinded to the identities of the samples. Compared samples were collected and analyzed under the same conditions.

Reporting for specific materials, systems and methods

Materials & experimental systems

n/a	Involvement in the study
<input type="checkbox"/>	<input checked="" type="checkbox"/> Unique biological materials
<input type="checkbox"/>	<input checked="" type="checkbox"/> Antibodies
<input checked="" type="checkbox"/>	<input type="checkbox"/> Eukaryotic cell lines
<input checked="" type="checkbox"/>	<input type="checkbox"/> Palaeontology
<input type="checkbox"/>	<input checked="" type="checkbox"/> Animals and other organisms
<input type="checkbox"/>	<input checked="" type="checkbox"/> Human research participants

Methods

n/a	Involvement in the study
<input checked="" type="checkbox"/>	<input type="checkbox"/> ChIP-seq
<input type="checkbox"/>	<input checked="" type="checkbox"/> Flow cytometry
<input checked="" type="checkbox"/>	<input type="checkbox"/> MRI-based neuroimaging

Unique biological materials

Policy information about [availability of materials](#)

Obtaining unique materials DEL-1-Fc, DEL-1[E1-E3]-Fc and DEL-1[RGE]-Fc proteins are available by the corresponding authors upon request.

Antibodies

Antibodies used

Antibodies against CD11b (clone M1/70, 1/100 dilution, catalog number: 552850, BD Biosciences), Ly-6G (clone 1A8, 1/100 dilution, catalog number: 551461, BD Biosciences), CD115 (clone AFS98, 1/100 dilution, catalog number: 12-1152-81, eBioscience), ICAM2 (CD102, clone 3C4 (mIC2/4), 1/100 dilution, catalog number: 557444, BD Biosciences) and F4/80 (clone BM8, 1/100 dilution, catalog number: 17-48-01-80, eBioscience) were used for flow cytometry. Antibody against mouse CD16/32 was used to block Fcγ receptors (clone 2.4G2, 1/100 dilution, catalog number: 553141, BD Biosciences). For in vivo functional inhibition assays a blocking antibody against CD11b (clone M1/70, 50µg/mouse, catalog number: 101214, Biolegend) was used. For in vitro intervention assays, a blocking antibody against CD11b (clone M1/70, final concentration 10µg/ml, catalog number: 101214, Biolegend), antibody against ICAM-1 (clone YN1/1.7.4, final concentration 10µg/ml, catalog number: 116110, Biolegend) or antibody against LFA-1 integrin (clone 17/4, final concentration 10µg/ml, catalog number: 101109, Biolegend) were used. An antibody against Ly6G (clone RB6-8C5, final concentration 5µg/ml, catalog number: 14-5931-81, eBioscience) and a secondary antibody (1/500 dilution, catalog number: A-11006, Invitrogen) were used for immunostaining of gingival tissues.

Validation

The antibodies are from commercial sources and have been validated by the vendors.

Animals and other organisms

Policy information about [studies involving animals](#); [ARRIVE guidelines](#) recommended for reporting animal research

Laboratory animals

Mice were housed under specific pathogen-free conditions on a standard 12/12h light/dark cycle. 8-10 weeks old sex-matched mice were used. Food and water were provided ad libitum. In experiments where only wild-type C57BL/6 mice were used, these were purchased from Janvier Labs or the Jackson Laboratory. Del1KO mice and mice overexpressing DEL-1 in the endothelium (EC-Del1) have been previously described. Mice overexpressing in macrophages full-length DEL-1 (CD68-Del1) or the truncated version of DEL-1 that lacks the discoidin I-like domains (CD68-Del1-[E1-E3]) were generated in C57BL/6N background, using the human CD68 promoter. Mice deficient in both LXR isoforms (Nr1h3KONr1h2KO; here referred to as Lxra-LxrbDKO) in a C57BL/6 background were originally provided from D. Mangelsdorf (University Texas Southwestern). Mice deficient in α L integrin (ItgalKO) or α M integrin (ItgamKO) were previously described. Mice deficient in beta3 integrin (Itgb3KO) and their respective wild-type control mice were from the Jackson Laboratory.

Wild animals

N/A

Field-collected samples

N/A

Human research participants

Policy information about [studies involving human research participants](#)

Population characteristics

All subjects were 28 years of age or older with no serious medical illness contraindicative of periodontal treatment. Gingival crevicular fluid was collected from 7 patients (3 males and 4 females) prior to initiation of scaling and root planing and at a reevaluation appointment 6 weeks later.

Recruitment

The inclusion criteria for chronic periodontitis were diseased sites with probing pocket depth \geq 5 mm associated with clinical attachment loss \geq 4 mm, presence of bleeding on probing, and radiographic evidence of bone loss.

Flow Cytometry

Plots

Confirm that:

- The axis labels state the marker and fluorochrome used (e.g. CD4-FITC).
- The axis scales are clearly visible. Include numbers along axes only for bottom left plot of group (a 'group' is an analysis of identical markers).
- All plots are contour plots with outliers or pseudocolor plots.
- A numerical value for number of cells or percentage (with statistics) is provided.

Methodology

Sample preparation

Single cell suspensions were prepared from peritoneal exudates from mice. Erythrocytes were removed with RBC lysis buffer and then cells were used for staining.

Instrument

FACS Canto II, FACS Aria cell sorter

Software

FlowJo version 9.3.2

Cell population abundance

Purity of FACS-sorted samples was $>95\%$.

Gating strategy

MSU-inflammation model: After gating on the singlets, peritoneal neutrophils were identified as Ly-6G+CD11b+ cells. Apoptotic neutrophils were detected based on their positivity for Annexin V. Peritoneal monocytes/macrophages from MSU crystal-treated mice were defined as Ly-6G-CD11b+ cells after excluding the SSC high eosinophil population. Macrophages were identified and sorted as CD11b+F4/80+ cells from peritoneal fluids of untreated mice. Resident macrophages in peritoneal fluids of untreated mice were identified and sorted as CD115+ICAM2+ cells.

- Tick this box to confirm that a figure exemplifying the gating strategy is provided in the Supplementary Information.